# Tracking Performance of the GBT

Richard M. Prestage

10 November 2011

GBT Archive:
File: PROJECTS
Keys: PTCS, Antenna, Tracking

**Abstract**

The Ka-band receiver and CCB were used to perform careful peaks and a series of half-power tracks on strong calibrators. The resulting antenna performance may be characterized as a mean pointing offset and an rms tracking error. The average rss combination of these two values is 1.19”, just satisfying the usable performance criteria of $\sigma_2 < 1.7$” under benign night-time conditions.

Many scans show the signature of the antenna servo resonance in the astronomical data. Mitigating this effect in the servo would improve the rms tracking error.

Currently, the dominant source of error under typical observing strategies is the initial offset pointing. This may be due to systematic errors in the pointing model; poor performance of the “peak” process, or azimuth track effects. These possibilities should be investigated further.

## History

**71.1** 10 November 2011. Original version (Richard Prestage).

## Contents

## 1. Introduction

The total pointing error observed while tracking a source is a combination of any error in the initial offset pointing measurement, and the tracking error. The tracking error may be due to servo error, or motion of the tip of the feedarm, due to vibration or wind. The "half-power track" technique provides a powerful method of measuring an upper limit to the total tracking error in one coordinate during the scan. During project TPTCSPNT_111023, we performed a series of half-power tracks on bright calibrators, under calm weather conditions. These data were used to characterize the astronomical performance of the telescope, and investigate the various sources of error limiting this performance.

Previous such analyses have been performed by Constantikes (2003, PTCS/PN/13.1), Balser and Prestage (2003, PTCS/PN/19.1), Balser et al (2006, PTCS/PN/49.1) and Ries et al (2009, PTCS/PN/64.4). The goals of this experiment were:

- to characterize the performance of the antenna after the azimuth track replacement, and with a more up-to-date azimuth track and pointing model, and
- to characterize the performance of the current servo as the "before" data before the antenna servo was upgraded.

## 2. Method

Astronomical data was acquired using the Ka-band receiver and the Caltech Continuum Backend (CCB). Data were logged under project TPTCSPNT_111023, and acquired from 01:25 to 08:00 UT on 2011/10/24. Observations were executed using the scheduling block ccbHalfPower.sb (Appendix 1). This performed the following actions:

- Calibrate on a bright, target calibrator:
  - peak, focus, repeat peak
  - track for 20 seconds on each of five positions offset by 0.0, 0.4, 0.5, 0.6 and 10 x FWHM, in either Azimuth or Elevation
- peak and focus on a "typical" near-by pointing calibrator
- slew directly to the half-power point (for 34.75 GHz) in Azimuth or Elevation of the target calibrator
- track that position for 15 minutes.

The target calibrators were chosen to have a range of azimuths and elevations.

The CCB was configured in the standard manner, with the cals firing, for the peak, focus and calibrator scans. For the target scans, the calibrator was turned off. The Archivist was used to record Quadrant Detector and Antenna Servo Error data, simultaneously with each observation.

The weather throughout the observing run was very stable, with calm winds (typically 0.5 m/s, and never exceeding 2 m/s), so we do not expect wind to play a signficant role in the results. Temperatures varied slowly between 4°C and 1°C, and there was uniform thin, high cloud. The resulting data quality was excellent.

## 3. Observations

Information on the observations made of the target calibrators is listed in Table 1.

| Scan | Source | $S$(0.9 cm) (Jy) | Calibrator | Azimuth (Degrees) | Elevation (Degrees) | Az Rate (“/sec) | El Rate (“/sec) | Offset |
|---|---|---|---|---|---|---|---|---|
| 64 | 2253+1608 | 16.67 | 2253+1942 | 191.622 | 67.422 | 33 | -5 | AZ |
| 84 | 2253+1608 | | | 209.079 | 65.347 | 30 | -5 | EL |
| 104 | 0319+4130 | 10.82 | 0310+3814 | 70.013 | 55.256 | 4 | 11 | AZ |
| 124 | 0319+4130 | | | 71.619 | 60.957 | 3 | 11 | EL |
| 146 | 0319+4130 | | | 72.677 | 67.035 | 0 | 11 | EL |
| 166 | 0319+4130 | | | 72.518 | 72.872 | -3 | 11 | AZ |
| 186 | 0927+3902 | 3.87 | 0929+5013 | 50.413 | 13.406 | 8 | 9 | AZ |
| 211 | 0927+3902 | | | 54.999 | 19.295 | 7 | 9 | EL |
| 231 | 0237+2848 | 3.42 | 0232+2628 | 238.018 | 73.949 | 27 | -10 | AZ |
| 251 | 0237+2848 | | | 250.585 | 68.468 | 17 | -10 | EL |
| 272 | 0423-0120 | 3.13 | 0422+0219 | 187.893 | 49.994 | 24 | 0 | AZ |

Table 1: The list of half-power scans obtained. The columns are as follows: *Column 1*.—Scan number for the half-power track scan. *Column 2*.—Source Name *Column 3*.—0.9mm flux density from the Ka-band pointing catalog. *Column 4*.—Name of the “typical” pointing calibrator. *Column 5*.—Azimuth of the observation. *Column 6*.—Elevation of the observation. *Column 7*.—Azimuth rate during the observation (estimated from the CLEO antenna display). *Column 8*.—Elevation rate during the observation (estimated from the CLEO antenna display). *Column 9*.—Direction of the half-power offset.

An attempt was made to observe 1923-2104 as it was setting, but the source had reached too low an elevation before useful tracking data could be obtained. Data for this source were used for the Offset Pointing analysis (Section 7.4) but were excluded from the tracking analysis.

## 4. CCB Data Analysis

We follow the method described in PTCS/PN/19 (Balser and Prestage 2003).

Assume that the antenna power pattern when convolved with a point source on the sky is a two-dimensional Gaussian. The antenna temperature in one direction is then given by:

$$T = T_{\rm src} \exp(-4 \ln 2 (x/\Theta)^2) \tag{1}$$

where $T_{\rm src}$ is the peak antenna temperature of the source, $x$ is the position on the sky, and $\Theta$ is the FWHM. The slope of the Gaussian evaluated at the half-power point is:

$$[dT/dx]_{x=\Theta/2} = M = -4\ln 2(T_{\rm src}/\Theta)\exp(-\ln 2) = -1.39(T_{\rm src}/\Theta) \tag{2}$$

Data were analysed as follows. The 34.75 GHz channels only of the CCB was used; the four phases were combined to provide switched power (in counts), and the port J10 (Beam 1 Y polarization) and J14 (Beam 2 X polarization) data were averaged together. The data were processed using python, and the numpy statistical package was used to calculate means, standard deviations, and power spectra.

The data in counts were converted to pointing offsets in arseconds as follows. Let the signal obtained from the on-source calibration scan be $T_0$. Since the telescope was still settling at the start of the scan (see later), the mean value from 10 - 20 seconds in the scan was used. Let the mean value of the 10 FWHM scan be $T_{\rm sky}$. Let $T(t)$ be the signal in counts while tracking at time t, and $P(t)$ the corresponding pointing error.

Then:

$$T_{\rm src} = T_0 - T_{\rm sky} \tag{3}$$

$$P(t) = M \times (T(t) - T_{\rm src}/2.0 - T_{\rm sky}) \tag{4}$$

The 0.4, 0.5 and 0.6 FWHM scans were not used directly in the analysis, but the 0.4 and 0.6 FWHM scans were used to derive a sanity check on the conversion scale $M$.

The data for a typical set of calibration plus target observations is listed in Table 2, and the tracking error as a function of time is shown in Figure 1.

| | | | |
|---|---|---|---|
| On Source Mean: | 2106.191 | RMS: | 11.855 |
| 0.4 FWHM Mean: | 1349.659 | RMS: | 93.741 |
| 0.5 FWHM Mean: | 1089.779 | RMS: | 90.901 |
| 0.6 FWHM Mean: | 833.801 | RMS: | 92.805 |
| Sky Mean: | 15.909 | RMS: | 0.538 |
| 0.5 FWHM Value: | 1073.870 | RMS: | 90.901 |
| Half Peak Value: | 1045.141 | RMS: | 5.927 |

0.4 - 0.6 FWHM Scale: -120.705 ± 30.865 Counts/arcsec
$T_{\rm src}$ Scale: -135.971 ± -0.771 Counts/arcsec
Tracking Data Mean: -0.697 ± 0.808”

Table 2: Output of the analysis program for scans 114-118 and 124

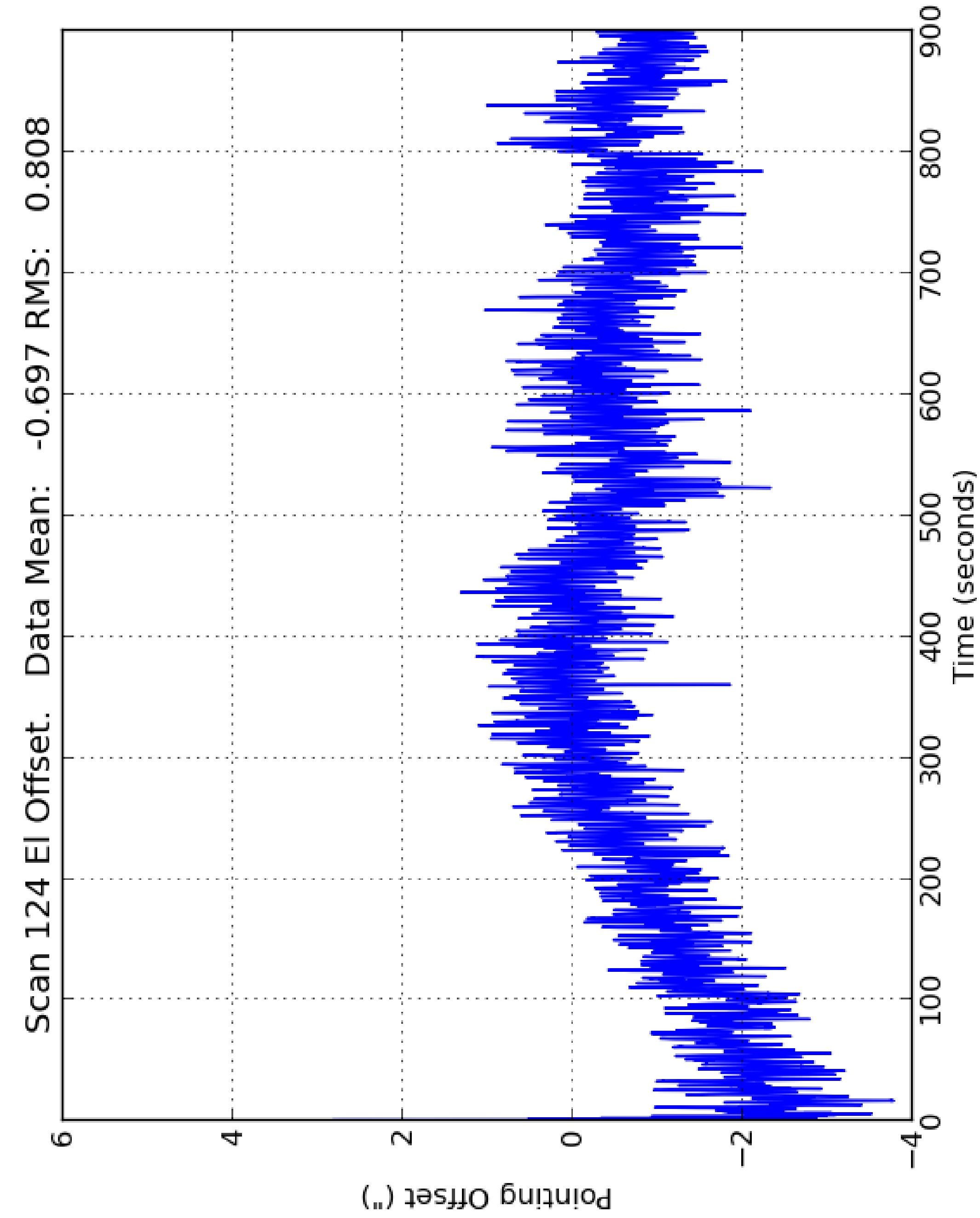


Fig. 1.— Pointing Error as a function of time for a “typical” El Offset, Scan 124

## 5. Antenna Servo Data

As noted, the Archivist was used to record the Antenna Azimuth and Elevation servo errors, logged at the rate of 50 Hz. The data for each calibration and target scan was inspected visually, and the following kinds of behavior were noted:

### 5.1. Azimuth

*Good Data*. For many scans, the azimuth tracking error was quite good, see Figure A1 for a typical example. The plot shows a mean tracking error of 0.0”, the toggling of an individual bit, and a slow variation with an rms error of 0.24”.

*Poor data*. For approximately half of the scans (32 of 65) (See Figure A2 for a typical example), the azimuth servo error would “wander” on timescales of a few seconds,with peak-peak errors ranging from a few to $\sim$ ten arcseconds.

*“Weird” data*. For a few scans (6 of 65) the azimuth servo would show large overshoot and ripple, with peak-peak errors a few tens of arcseconds (Figure A3).

*Zero-crossing data*. For one scan (146) the azimuth rate crossed from positive to negative, approximately 300 seconds into the scan. This results in a “glitch” in the azimuth servo error, presumably due to sticktion or some other zero-velocity behavior of the servo (see Figure A4). (This glitch is not present in the corresponding elevation servo error.)

*Half-power track scans.* A typical AZ half-power track scan is shown in Figure A5.

### 5.2. Elevation

*Good data*. For a number of scans, the elevation pointing error looked quite good, with a mean error of zero, and an rms of $\leq$ 0.7”. See Figure A6 for a particularly good example.

*Overshoot*. For many (all?) scans where the antenna was not tracking close to the start of the scan, the elevation servo error shows the antenna initially off-source at the start of the scan, with a $\sim$ five arcsecond overshoot, before settling on the source position after $\sim$ five seconds (Figure A7).

*Periodic oscillations*. For a majority of scans (45 of 65) there are obvious periodic oscillations in the data, with rms values around 0.4 - 0.6”, peak-to-peak values around $\pm$ 0.5 - 1”, and periods around three to seven seconds of time. Examples are shown in Figures A8 and A9.

*Half-power track scans*. All the EL half-power track scans show the initial overshoot, and periodic oscillations. Good and poor examples are shown in Figures A10 and A11.

### 5.3. Servo performance during peak scans

Although not subjected to a rigorous analysis, a casual perusal of the antenna performance during “peak” scans showed essentially similar behavior to that described above.

## 6. Quadrant Detector Data

The quadrant detector output for the calibration scans also displays a variety of behavior as follows:

### 6.1. Cross-elevation

*Initial disturbance.* Essentially all scans where the telescope has to move to arrive on source show at least an initial disturbance at the beginning of the scan. An example is shown in Figure B1.

*Flat scans.* For all of the scans where the telescope is close to on source (i.e. the 0.4, 0.5 and 0.6 FWHN scans), the quadrant detector output is essentially flat (Figure B2).

*Ringing*. For the majority of the 10 FWHN scans (but not the 0 FWHM scans), the quadrant detector data exhibits ringing throughout the scan, with peak-to-peak amplitudes ranging from a few to $\sim$ eight arcseconds peak-peak. A particularly obvious example is shown in Figure B3.

*Half-power tracks.* For 8 of 11 half-power tracks, the quadrant detector data are either flat, or show slow drifts of less than $\sim$ two arcseconds. (Figure B4). The remaining three show linear drifts of $\sim$ five arcseconds (Figure B5).

### 6.2. Elevation

*Initial disturbance.* As for cross-elevation, for all scans where significant telesocpe motion is required, the quadrant detector elevation show a large peak at the start of the scan (Figure B6).

Unlike for cross-evelation, the elevation data show no signs of strong ringing.

*Half-power tracks*. All of the elevation data show slow drifts of two arcseconds or less, apart from Scan 146, which shows a 10” linear drift (Figure B7).

## 7. Results

### 7.1. Astronomy Data - Spectral Features

All of the half-power tracks were inspected by eye as both time series and power spectra. Some obvious spectral features are listed in Table 3.

A power spectrum of scan 186, which shows most of the above features, is shown in Figure 2.

### 7.2. Antenna Servo Resonances

As is now well known - see Memo “Resonances in the GBT Servo System point to the motors” (Weadon 2009) [1] - both azimuth and elevation axes of the GBT show “servo resonances” with frequencies around

[1] /home/doc/gbt/subsys/servo/ArchivedDocuments/ElevationServoResonances2009/ElResonancesV4

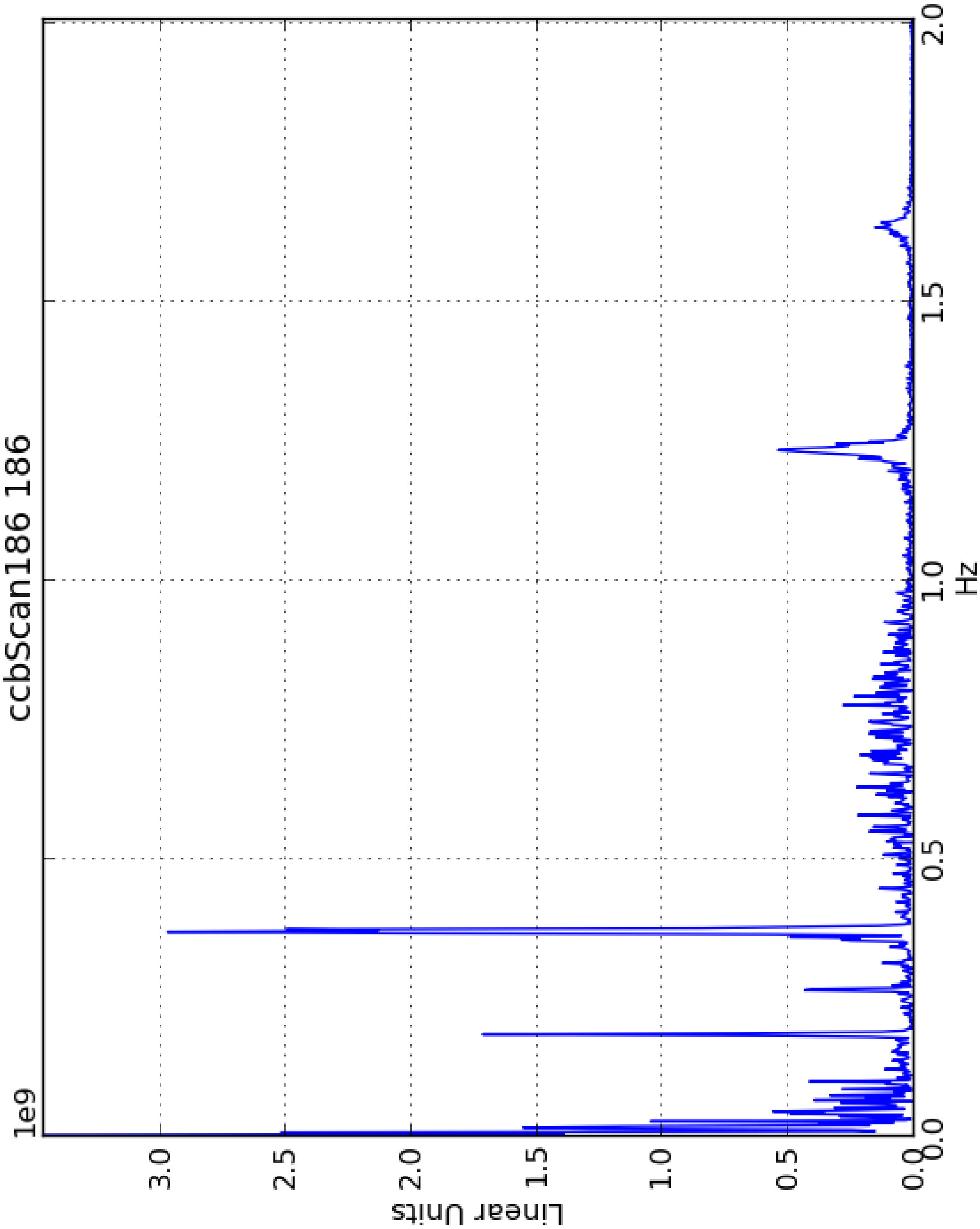


Fig. 2.— CCB Data for AZ scan 186 - power spectrum

| Scan | Offset | Frequencies |
|---|---|---|
| 64 | AZ | 0.86Hz, 1.22Hz, 1.7-1.75Hz comb, no obvious servo resonance |
| 84 | EL | 0.33 - 0.38Hz comb, no obvious servo resonance |
| 104 | AZ | 1.22 Hz, no obvious servo resonance |
| 124 | EL | 0.282 Hz (fundamental), 0.567 Hz (2nd harmonic) |
| 144 | EL | 0.283 Hz (fundamental), 0.566 Hz (2nd harmonic) |
| 166 | AZ | 0.648 Hz, 1.24 Hz, no obvious servo resonance |
| 186 | AZ | 0.184 Hz (2nd harmonic), 0.264 Hz (3rd), 0.367 Hz (4th) 1.23Hz 1.63Hz |
| 211 | EL | 0.0132 Hz, 0.497 Hz (3rd harmonic) |
| 231 | AZ | 1.24 Hz, no obvious servo resonance |
| 251 | EL | 0.286 Hz (fundamental), 0.571 Hz (2nd harmonic) |
| 272 | AZ | 1.23 Hz, 1.62 - 1.67Hz comb, no obvious servo resonance |

Table 3: Obvious spectral features in the half-power track astronomy data.

a few tenths of an arcsecond. These are now understood to be caused by the DC brush motors; the resonances are a function of motor speed, and hence of antenna rate (16"/sec corresponds to 0.194Hz in azimuth and 0.389Hz in elevation, respectively).

An example of the antenna elevation servo error is show in Figures 3 and 4 (time series) and 5 and 6 (power spectra). The fundamental and second, third and fourth harmonics for a rate of 11.8"/sec are obvious in the data.

Corresponding plots for the CCB data are shown in figures 7 and 8 (time series) and 9 (power spectrum).The fundamental and second harmonic are clearly visible in the data.

Similar effects are visible in Azimuth - see figures 10 for the antenna servo error data, and figure 11 and for the CCB data. Finally, Figure 12 showns the Quadrant Detector cross-elevation for Scan 186. The peaks at 1.22 and 1.63Hz are clearly visible.

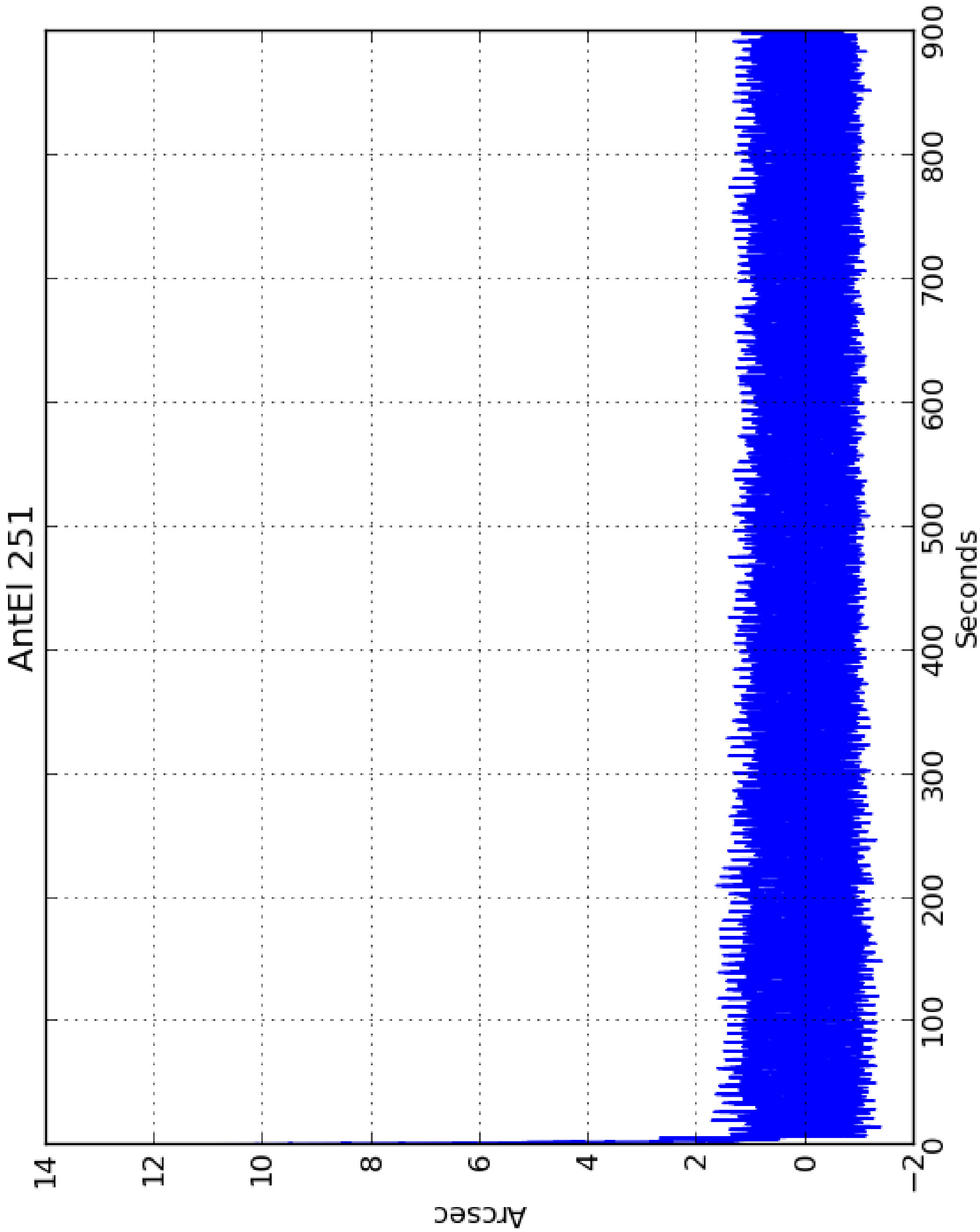


Fig. 3.— Elevation Servo Error for scan 251

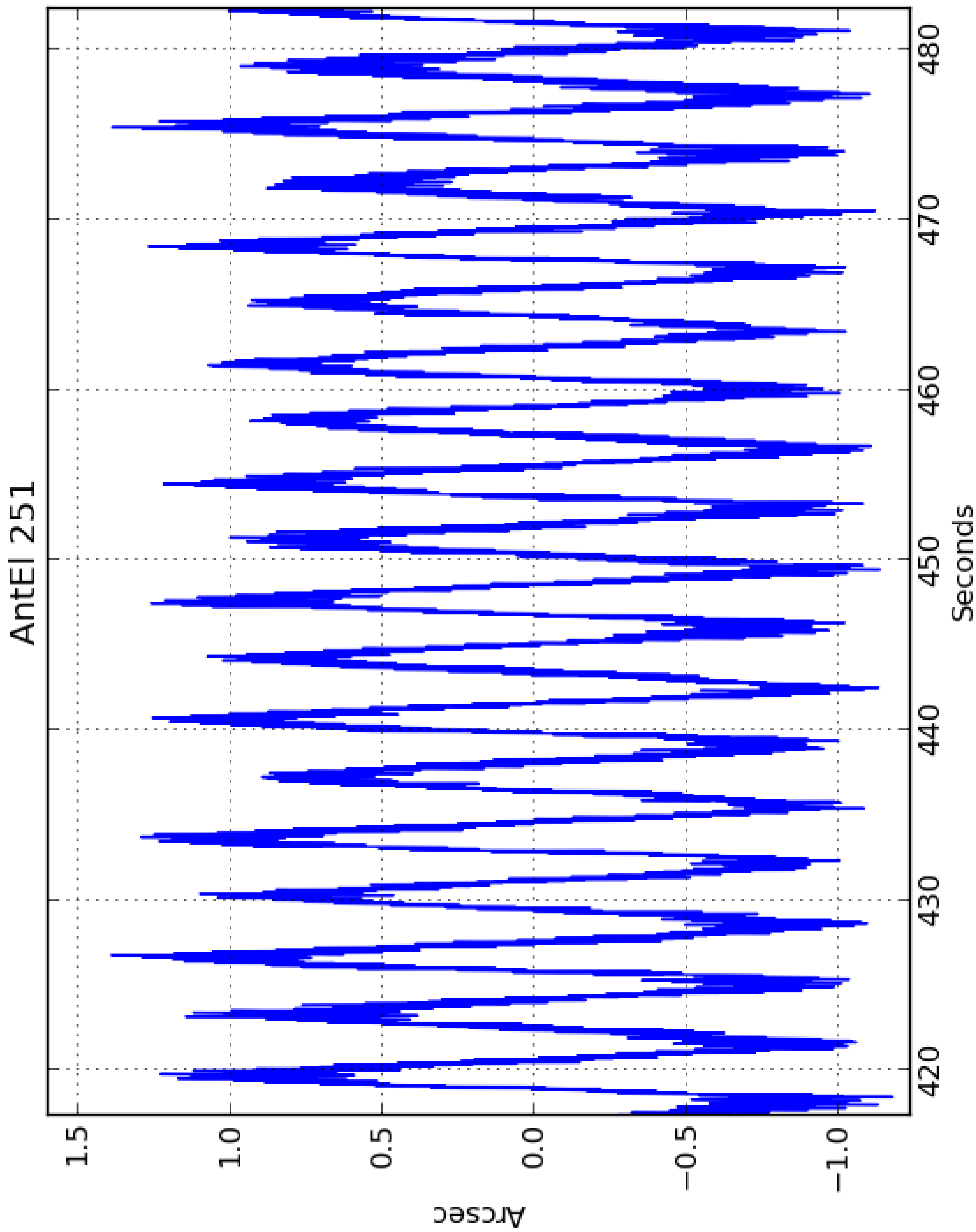


Fig. 4.— Elevation Servo Error for scan 251 - expanded time scale

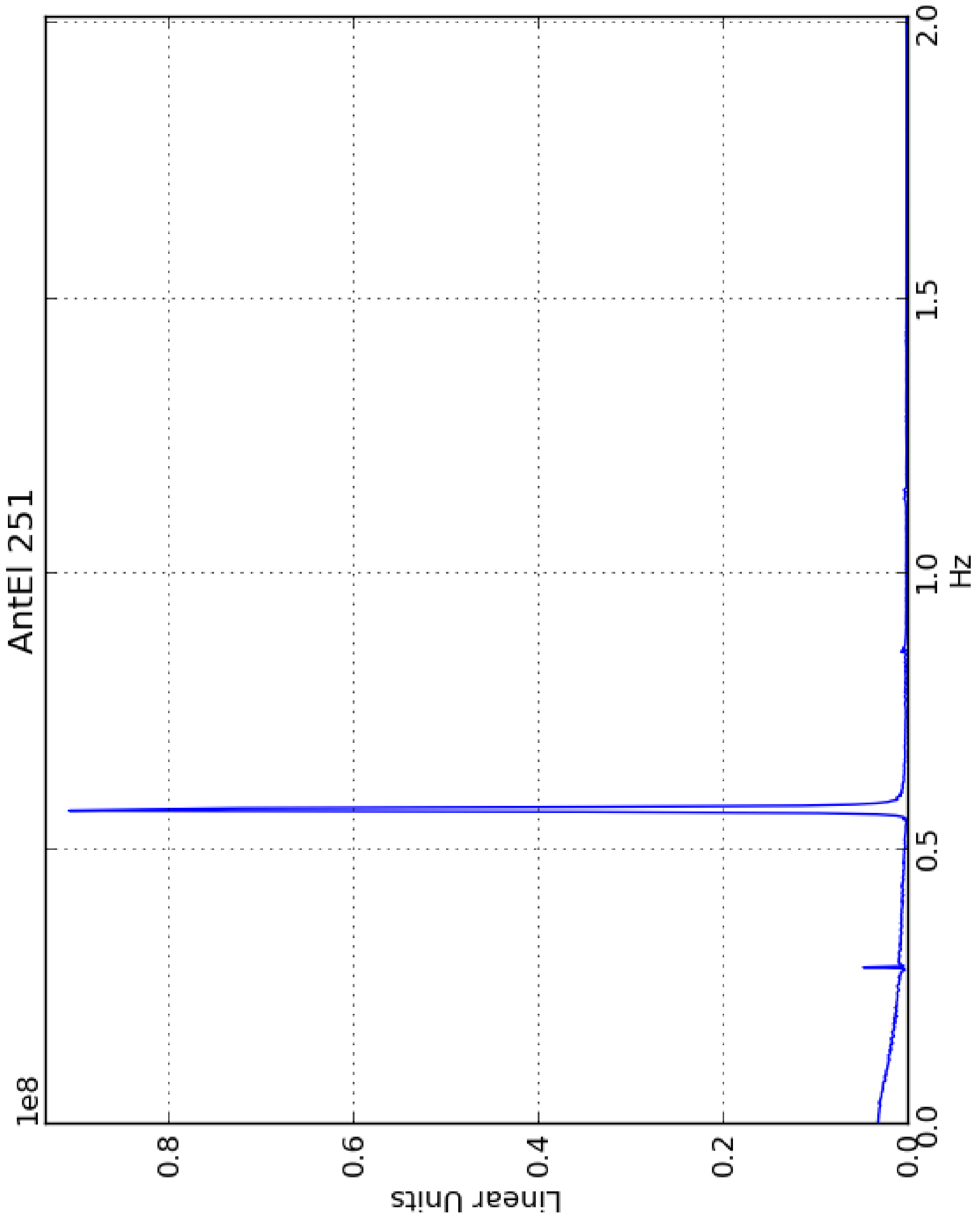


Fig. 5.— Elevation Servo Error for scan 251 - power spectrum

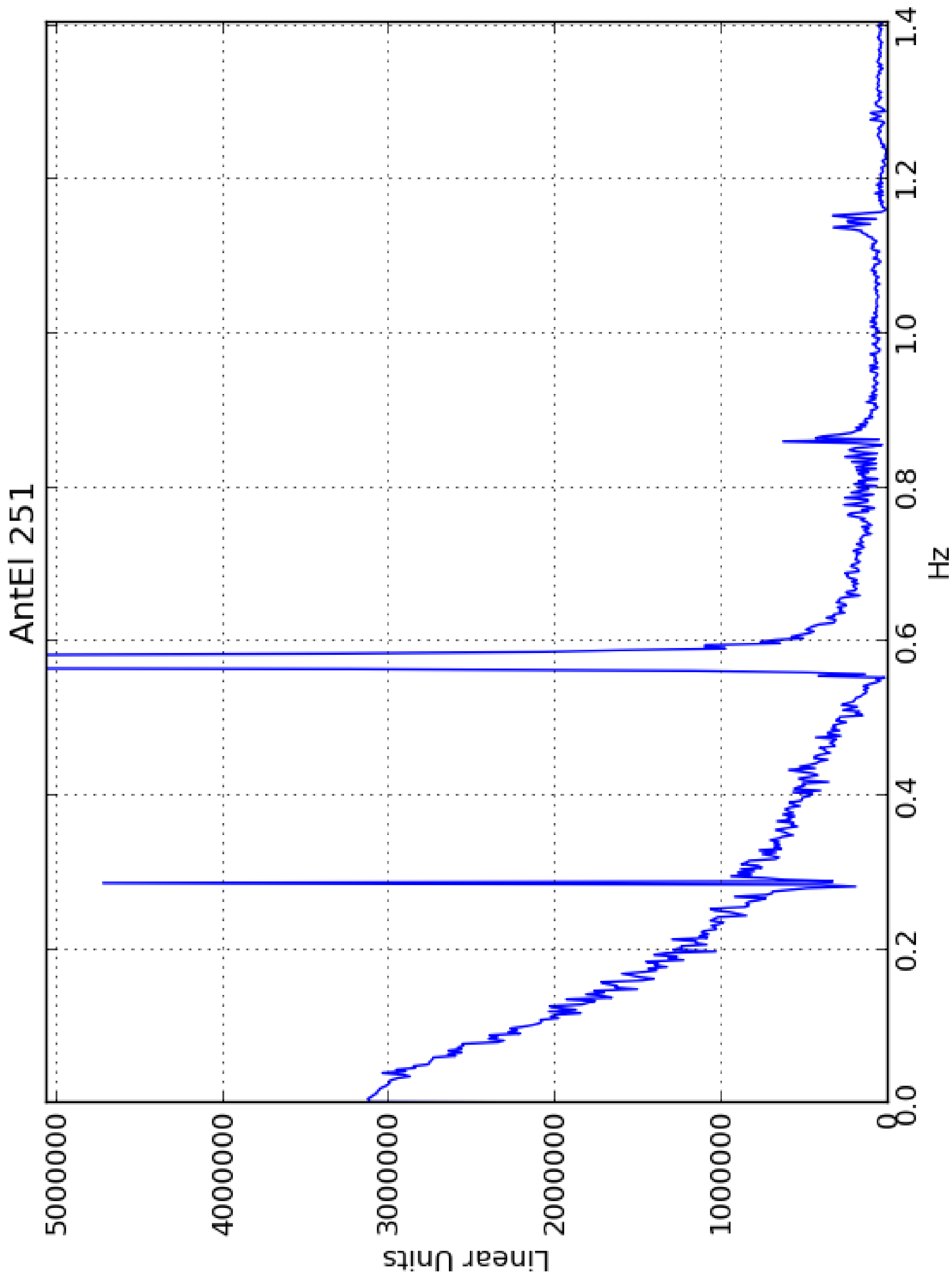


Fig. 6.— Elevation Servo Error for scan 251 - expanded frequency scale. Resonances are at 0.287, 0.571, 0.858 and 1.148Hz, corresponding to the fundamental, second, third and fourth harmonics for an elevation rate of 11.8"/sec.

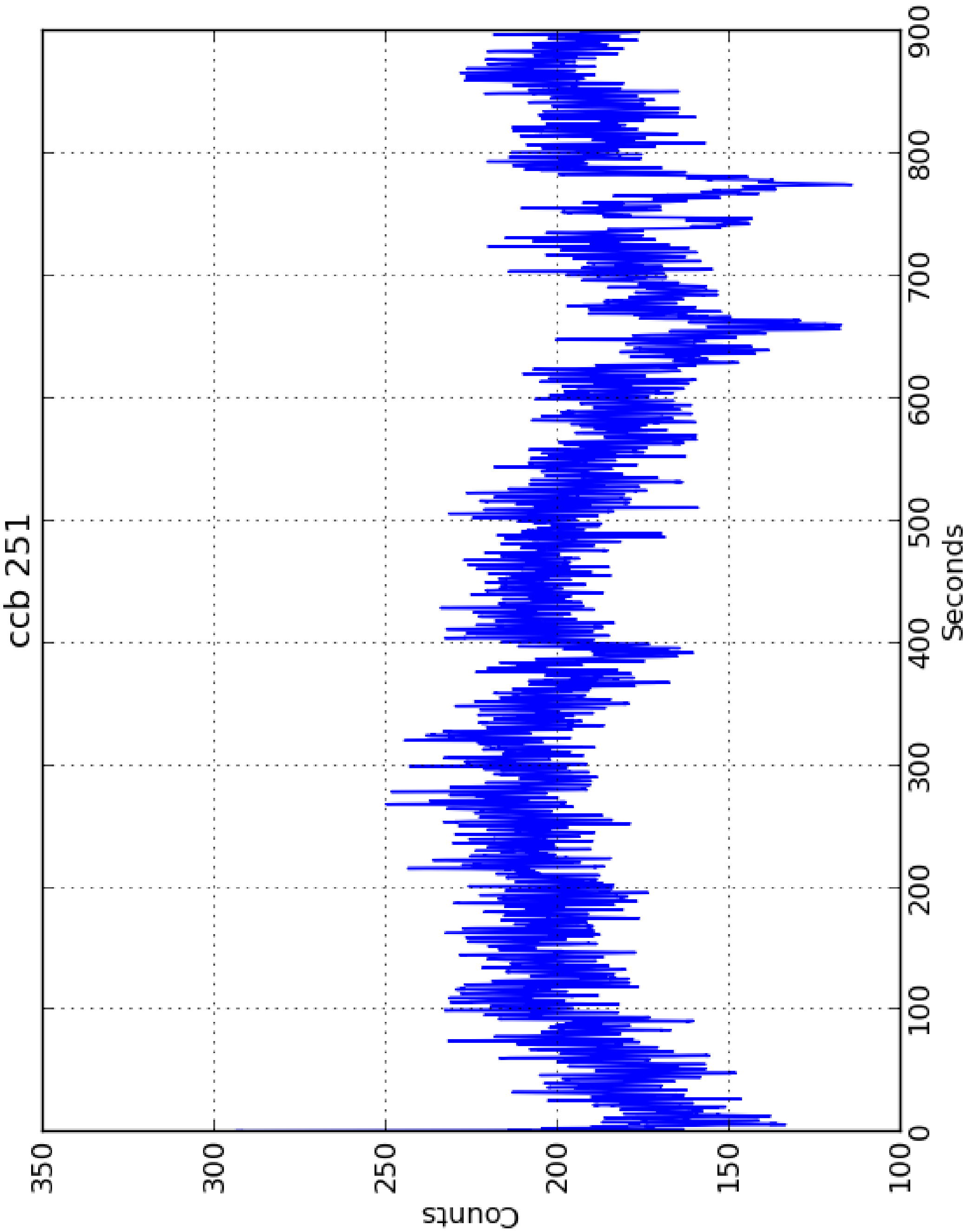


Fig. 7.— CCB data for scan 251

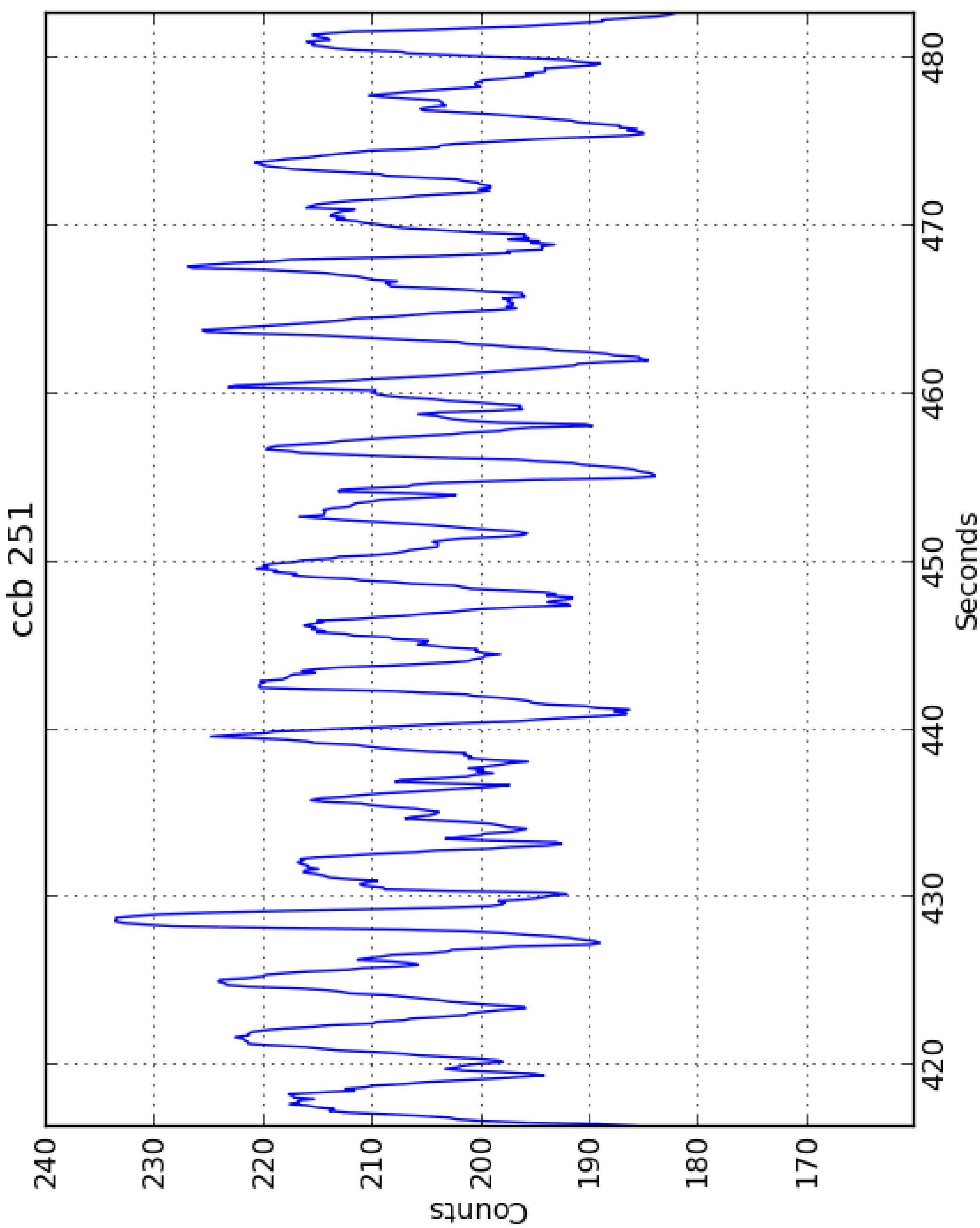


Fig. 8.— CCB data for scan 251 - expanded time scale

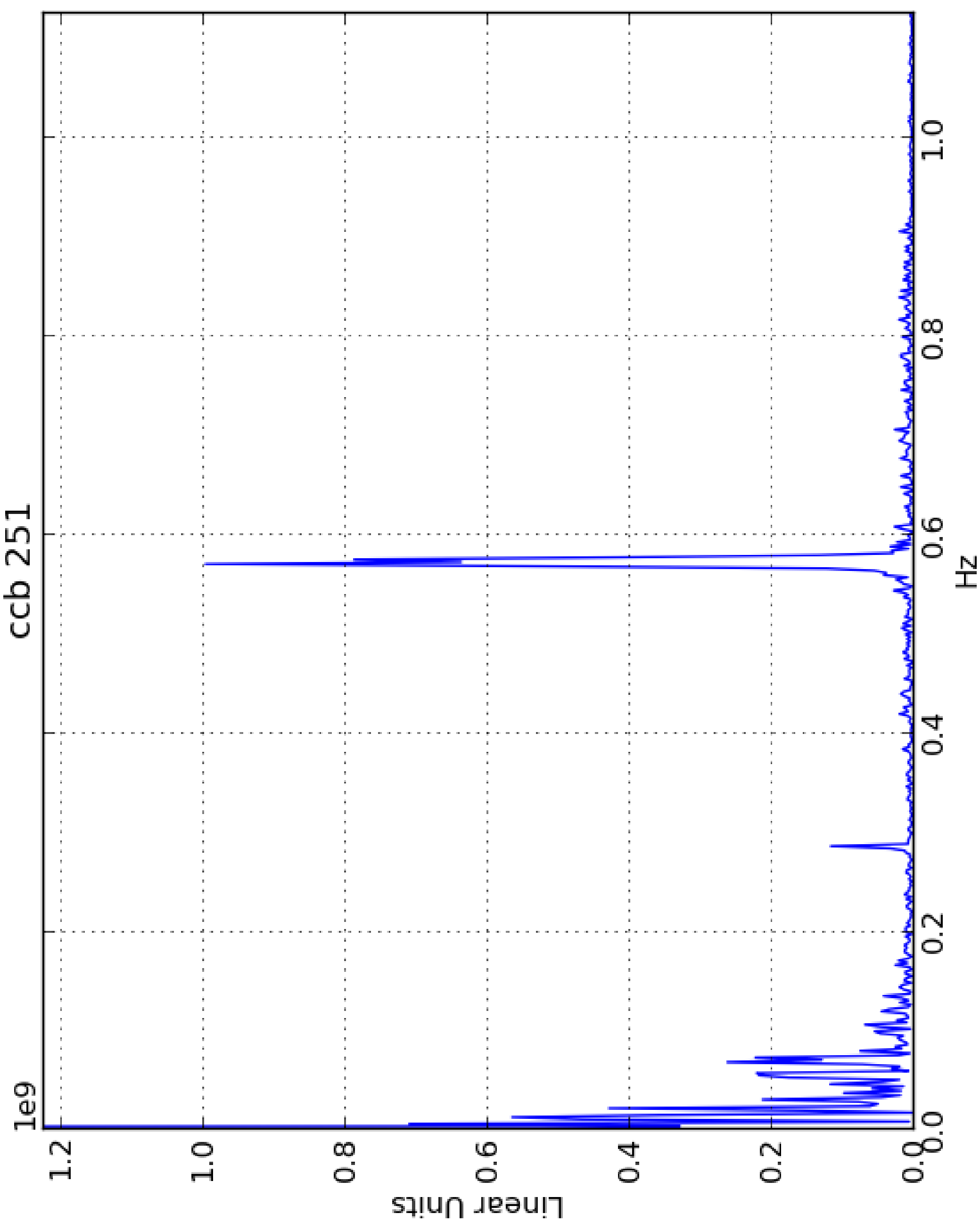


Fig. 9.— CCB data for scan 251 - power spectrum

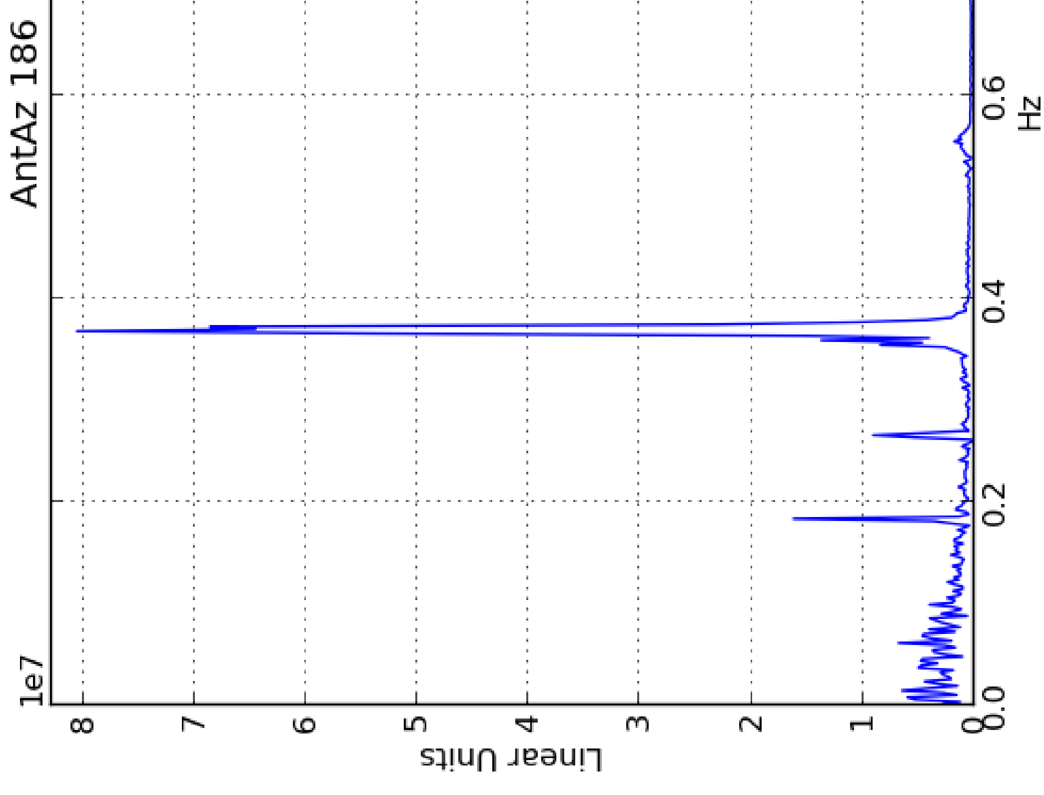


Fig. 10.— Elevation Servo Error for scan 186 - expanded frequency scale. Resonances are at 0.182, 0.263, and 0.367Hz, corresponding to the first second and third harmonics for an azimuth rate of 8.5"/sec.

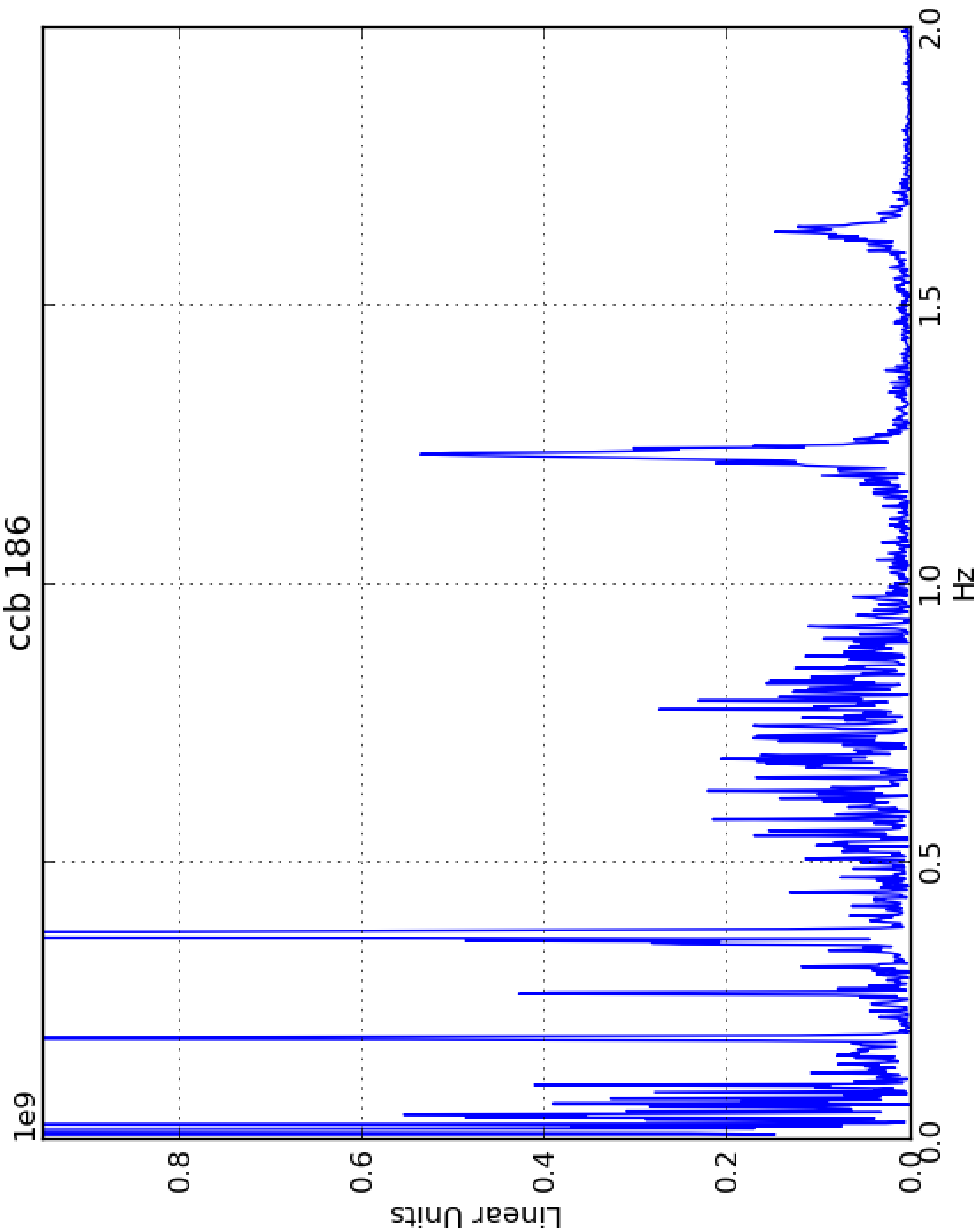


Fig. 11.— CCB data for scan 186 - expanded frequency scale. Resonances are at 0.182, 0.263, and 0.367Hz, corresponding to the first second and third harmonics for an azimuth rate of 8.5”/sec. Peaks are also obvious at 1.22 and 1.63 Hz.

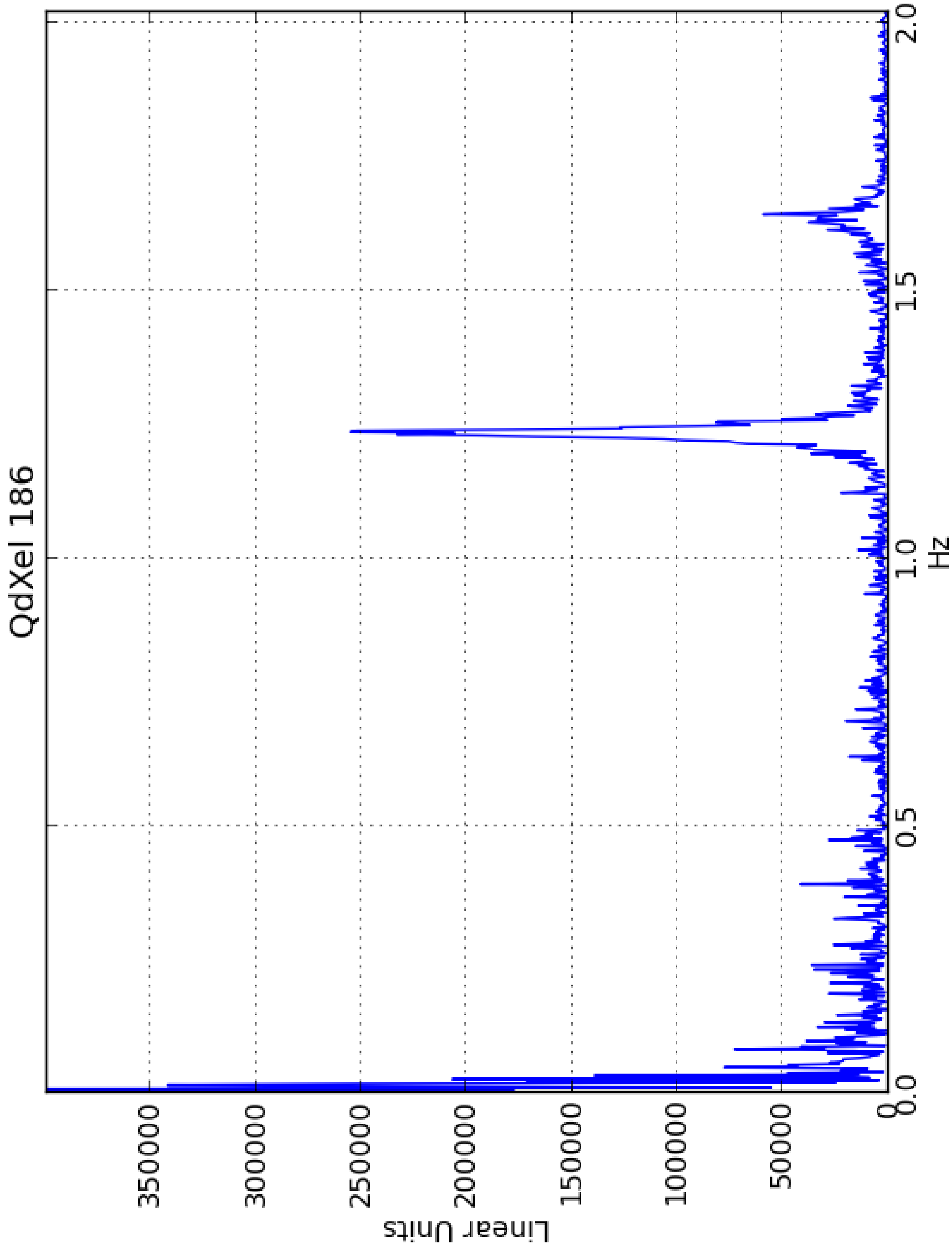


Fig. 12.— Quadrant Detector data for scan 186 - expanded frequency scale. Peaks are obvious at 1.22 and 1.63 Hz.

### 7.3. Offset Tracking Performance

The offset tracking data for all eleven scans are shown in Appendix D. Note no linear baselines or even DC offsets have been removed from these data; they are directly the result of applying Equation (4) to the data.

The mean tracking offset, and rms tracking error for the 11 half-power tracks is given in Table 4. The performance is similar for both azimuth and elevation. The "Mean Offset" corresponds to how well the offset pointing has located the telescope, while the "RMS tracking Error" quantifies how well the telescope tracks the target once it has been acquired.

The rms of the mean offsets is 0.86". The average of the rms tracking error values is 0.88" $\pm$ 0.15"; the average of the RSS errors is 1.19" $\pm$ 0.46".

| Scan | Offset Direction | Mean Offset | RMS Tracking Error | RSS (Total Offset) |
|---|---|---|---|---|
| 64 | AZ | 0.11 | 0.95 | 0.96 |
| 84 | EL | -2.29 | 0.89 | 2.46 |
| 104 | AZ | 1.06 | 0.84 | 1.35 |
| 124 | EL | -0.70 | 0.81 | 1.07 |
| 146 | EL | -0.92 | 0.69 | 1.15 |
| 166 | AZ | 0.30 | 0.70 | 0.77 |
| 186 | AZ | -0.05 | 1.11 | 1.11 |
| 211 | EL | -1.06 | 1.11 | 1.53 |
| 231 | AZ | 0.23 | 0.67 | 0.71 |
| 251 | EL | 0.20 | 0.90 | 0.92 |
| 272 | AZ | -0.08 | 1.03 | 1.03 |

Table 4: Mean Offset, RMS Tracking Error and RSS of these two quantities for the half-power track scans

### 7.4. Offset Pointing Performance from Peak Scans

Although rather few in number, the careful peak scans performed during the run allow us to investigate the offset performance of the antenna in two additional ways:

- the difference between the two peaks performed on each target calibrator should provide an estimate of the "best" offset pointing possible, with no time delay and no change of target source between observations.
- the difference between the peaks performed on the target calibrators and peaks performed on the "typical" calibrators provide an estimate of the performance for a "typical" slew (close pointing

source and target calibrator) on the sky and a large slew on the sky (target calibrator to next pointing source), with approximately 10 - 20 minutes of time between successive peaks.

These results are given in Tables 5 and 6 respectively.

| Scan | Source | Azimuth (Degrees) | Elevation (Degrees) | Az Rate ("/sec) | El Rate ("/sec) | XEL " | EL " |
|---|---|---|---|---|---|---|---|
| 6 | 1924-2914 | 217.454 | 11.371 | 32.891 | -6.044 | 0.120 | 0.223 |
| 26 | 1924-2914 | 222.849 | 7.630 | 24.838 | -11.857 | -0.567 | -2.789 |
| 45 | 2253+1608 | 188.007 | 67.616 | 85.963 | -2.697 | 0.274 | 0.892 |
| 65 | 2253+1608 | 205.939 | 65.874 | 74.797 | -4.908 | -0.155 | 0.625 |
| 85 | 0319+4130 | 69.670 | 54.205 | 39.059 | 11.165 | -0.520 | -0.686 |
| 105 | 0319+4130 | 71.355 | 59.887 | 43.271 | 11.211 | -0.225 | -0.536 |
| 127 | 0319+4130 | 72.555 | 65.949 | 52.576 | 12.439 | 0.329 | 1.202 |
| 147 | 0319+4130 | 72.688 | 71.738 | 62.661 | 9.319 | 0.795 | -0.125 |
| 167 | 0927+3902 | 49.676 | 12.538 | 29.364 | 8.999 | -1.433 | 0.650 |
| 192 | 0927+3902 | 54.341 | 18.398 | 29.461 | 9.580 | 0.373 | 0.307 |
| 212 | 0237+2848 | 234.827 | 74.906 | 120.760 | -5.345 | 0.491 | -0.217 |
| 232 | 0237+2848 | 248.631 | 69.545 | 74.050 | -11.025 | 0.058 | 0.589 |
| 253 | 0423-0120 | 185.697 | 50.125 | 52.443 | -0.006 | -0.392 | -0.591 |

Table 5: Peak Offsets for Target Calibrators The columns are as follows: *Column 1*.—Scan number for first pointing scan. *Column 2*.—Source Name *Column 3*.—Azimuth of the observation. *Column 4*.—Elevation of the observation. *Column 5*.—Azimuth rate during the observation. *Column 6*.—Elevation rate during the observation. *Column 7*.—XEL pointing offset between the two azimuth peaks. *Column 8*.—EL pointing offset between the two elevation peak.

The mean pointing offset from repeat peaks on the target calibrators is 0.0" (as expected), with an rms of 0.557" in cross-elevation, and 0.980" in elevation.

The mean pointing offset using successive Pointing Source - Target Calibrator - Pointing Source observations is 0.104" with an rms of 2.639" in cross elevation, and -0.361" with an rms of 2.745" in elevation.

| Scan | Source | Azimuth (Degrees) | Elevation (Degrees) | Az Rate ("/sec) | El Rate ("/sec) | XEL " | EL " |
|---|---|---|---|---|---|---|---|
| 20 | 1923-2104 | 224.296 | 16.694 | 29.213 | -3.583 | 0.114 | 0.239 |
| 26 | 1924-2914 | 222.849 | 7.630 | 24.838 | -11.857 | -2.013 | -0.932 |
| 40 | 1923-2104 | 229.949 | 12.444 | 35.041 | -8.405 | -1.012 | -2.096 |
| 45 | 2253+1608 | 188.007 | 67.616 | 85.963 | -2.697 | 7.279 | -0.631 |
| 59 | 2253+1942 | 196.537 | 70.699 | 105.504 | -5.975 | -0.001 | -3.304 |
| 65 | 2253+1608 | 205.939 | 65.874 | 74.797 | -4.908 | 0.636 | 0.344 |
| 79 | 2253+1942 | 215.460 | 68.079 | 87.316 | -5.279 | 1.322 | -0.034 |
| 85 | 0319+4130 | 69.670 | 54.205 | 39.059 | 11.165 | -2.378 | -5.935 |
| 99 | 0310+3814 | 76.649 | 56.968 | 41.821 | 13.083 | 1.009 | -0.202 |
| 105 | 0319+4130 | 71.355 | 59.887 | 43.271 | 11.211 | 0.956 | 1.974 |
| 119 | 0310+3814 | 79.274 | 62.880 | 50.976 | 15.978 | -1.206 | 1.115 |
| 127 | 0319+4130 | 72.555 | 65.949 | 52.576 | 12.439 | 1.336 | 0.745 |
| 141 | 0310+3814 | 82.007 | 69.171 | 62.241 | 12.159 | -0.070 | -1.808 |
| 147 | 0319+4130 | 72.688 | 71.738 | 62.661 | 9.319 | -0.483 | -2.218 |
| 161 | 0310+3814 | 84.676 | 75.302 | 78.465 | 11.841 | -1.391 | -2.311 |
| 167 | 0927+3902 | 49.676 | 12.538 | 29.364 | 8.999 | -5.846 | 7.562 |
| 181 | 0929+5013 | 41.334 | 20.443 | 23.908 | 12.038 | 0.225 | -0.300 |
| 192 | 0927+3902 | 54.341 | 18.398 | 29.461 | 9.580 | 1.391 | 2.294 |
| 206 | 0929+5013 | 44.946 | 25.522 | 23.213 | 8.487 | 0.166 | -0.744 |
| 212 | 0237+2848 | 234.827 | 74.906 | 120.760 | -5.345 | 6.592 | -6.836 |
| 226 | 0232+2628 | 236.698 | 70.910 | 84.810 | -18.414 | -1.016 | -0.192 |
| 232 | 0237+2848 | 248.631 | 69.545 | 74.050 | -11.025 | 1.278 | 2.312 |
| 246 | 0232+2628 | 248.514 | 65.512 | 70.514 | -3.104 | -0.746 | 0.279 |
| 253 | 0423-0120 | 185.697 | 50.125 | 52.443 | -0.006 | -4.222 | -0.558 |
| 267 | 0422+0219 | 190.221 | 53.508 | 51.650 | -0.897 | 0.669 | 2.204 |

Table 6: Peak offsets for Target and Typical Calibrator Observations. The columns are as for Table 2.

## 8. Discussion

From these results the rms tracking error is typically 1" or better in each axis. On its own, this would satisfy the criterion for usable offset tracking at 86 GHz $\sigma_2 < 1.7$" (Condon 2003, PTCS/PN/27.2).

To this however must be added any error in the offset pointing. From these data, the average one-dimensional rss of the mean offset plus tracking error is 1.19". Assuming equal az and el contributions this would correspond to $\sigma_2 = 1.68$", just inside the usable value.

The offset pointing performance has also been calculated for careful repeat peaks on strong calibrators, and more typical observing. The former also provides usable performance, while the latter gives a one-dimensional offset pointing error of $\sim 2.7$".

Possibilities for this discrepancy include (a) systematic errors in the pointing model, which manifest as small residuals after large slews, (b) poorer performance of the "peak" process if the antenna servo and feed arm are still experiencing disturbances due to the large slew, and (c) azimuth track effects.

Disregarding the mean offset, the rms tracking error is very well behaved; no slopes in the astronomical data are present over timescales of 15 minutes, suggesting this pointing performance would extend to half an hour or longer under benign thermal conditions. Note that on a number of occasions the quadrant detector data show large drifts which are not apparent in the astronomical data, suggesting they are instrumental in origin (in any case, they appear quite non-physical). This will have implications for the use of the quadrant detector to correct for pointing errors due to motion of the feed arm.

Four of five EL scans and one of six AZ scans show obvious signs of the servo resonance, confirming earlier work that the effect is much more pronounced in elevation. Whenever the servo resonance is obvious in the antenna servo error, it is also readily apparent in the astronomical data, so addressing this problem would significantly improve the offset tracking performance.

In addition to the servo resonance, a number of scans show spectral features at 1.22 and 1.67 Hz. The former is a known structural resonance (see e.g. Ravichandran (2003, PTCS/PN/6.1). The latter is of unknown origin (to me). These features are also present in the Quadrant Detector data, so it might be possible to servo them out with the subreflector, if these frequencies are within its usable bandwidth.

Many of the twenty-second calibration scans show a variety of servo performance issues, in both azimuth and elevation; these are also present in many "peak" scans. Combined with occasional feed-arm ringing, this suggests that the present peak process may not be optimal, and alternative strategies (such as fivepoints or scanning in a circle at the half-power point) might be preferrable. These should be investigated.

## 9. Conclusions

The Ka-band receiver and CCB were used to perform careful peaks and a series of half-power tracks on strong calibrators. The resulting antenna performance may be characterized as a mean pointing offset and an rms tracking error. The average rss combination of these two values is 1.19", just satisfying the usable performance criteria of $\sigma_2 < 1.7$" under benign night-time conditions.

Many scans show the signature of the antenna servo resonance in the astronomical data. Mitigating this effect in the servo would improve the rms tracking error.

Currently, the dominant source of error under typical observing strategies is the initial offset pointing. This may be due to systematic errors in the pointing model; poor performance of the "peak" process, or azimuth track effects. These possibilities should be investigated further.

## 10. Achknowledgements

Thanks to Brian Mason for useful discussions, and assistance with the CCB data processing, and Frank Ghigo for assistance with the scheduling block and processing the peak data.

## A. ccbHalfPower.sb

```
# block to do tracks at the half-power point
# version for CCB  November 2007
# revised Oct 2011

# RMP 23 October 2011 switch catalog to kaband_pointing
# RMP 23 October 2011 use ccbptcs_nocal configuration for the tracks
# RMP 18 October 2011 call addwxqpa.py to include antenna in archivist
# RMP 18 October 2011 add initial Peak on target source (source2)
#------------------------------------
# remember to use the correct .sparrow file for CCB:
#  [GfmDataProcessingDefaults]
#  BeamSwitched: BeamSwitched
#  BeamSwitchedTBOnly: BeamSwitchedTBOnly
#  DualBeam: DualBeam
#  TotalPower: Raw
#  [Continuum]
#  Frequency: 34.75
#  Polarization: Y/Right
#------------------------------------

#------------------------------------------------------------------
# set specifications here
#  will peak on source1 and HP track on source2
#
# In detail:
#  AutoPeakFocus on source2
#  Repeat Peak on source2
#  Do the calibration scans on source2
#  AutoPeakFocus on source1 (simulating normal observing strategy
#  Do the half-power track on source2
#
#------------------------------------------------------------------
# source1 = "1256-0547"  # 3C279  about 21 Jy at Ku band
# source2 = "1256-0547"  # 3C279  about 21 Jy at Ku band
# source1 = "2253+1608"    # 3C454.3
# source1 = "0359+5057"
# source2 = "0319+4130"
# source1 = "2253+1942"
# source2 = "2253+1608"
# source1 = "1923-2104"
# source2 = "1924-2914"
#source1 = "0310+3814"
```

```
#source2 = "0319+4130"
#source1 = "0929+5013"
#source2 = "0927+3902"
#source1 = "0232+2628"
#source2 = "0237+2848"
source1 = "0422+0219"
source2 = "0423-0120"

direction = 'az'      # select az or el offsets
# direction = 'el'
freq = 34.75   # GHz  # used for HPBW calculation

trackdur = 15   # number of minutes for HP track

numtracks = 1     # number HP tracks after calibration
                  # will re-do the peak before each
#------------------------------------------------------------------

import os

# Add ptcs directory to the path so we can reference files as modules
ptcsturtledir = "/home/groups/ptcs/ccbobs/turtle"
sys.path.append(ptcsturtledir)

execfile(os.path.join( ptcsturtledir ,  "ccbptcssetup.py"))

# load catalogs
# Catalog(fluxcal)
Catalog(kaband_pointing)

# Calc half power offset
freq = 34.75             # best S/N channel
fwhm = 1.2 * 206265.0 * (3.0e8) / (100.0*freq*1.0e9)   # in arcsec

# function ofst creates an offset in units of the HPBW
def ofst(wf) :
  if direction == 'az' :
    return Offset("Encoder", (wf * fwhm/3600.0), 0.0)
  else :
    return Offset("Encoder", 0.0, (wf * fwhm/3600.0))

print 'fwhm, etc', fwhm, ofst(0), ofst(0.5)
```

```
Configure(ccbptcspnt2)
killlo()
undead()

# add archivist for weather, quad detector, etc
execfile('/home/groups/ptcs/ccbobs/turtle/addwxqpa.py')

Slew(source2)
# Balance()

# initial peak/focus on source2, repeat peak
AutoPeakFocus(source2, configure=False, balance=False, beamName="1")
AutoPeak(source2, configure=False, balance=False, beamName="1")
Break("Check peak/focus")

# calibrate offsets - direction az or el has been set above
for delpos in [0, 0.4, 0.5, 0.6, 10] :
  print 'offsets', delpos, ofst(delpos)
  Track(source2, None, 20, beamName="1", fixedOffset=ofst(delpos))

# now peak/focus on source1 to simulate normal observing

AutoPeakFocus(source1, configure=False, balance=False, beamName="1")

# tracks at azimuth half-power
while numtracks > 0 :

  Configure(ccbptcs_nocal)
  killlo()
  undead()

  print 'offset=',  ofst(0.5)
  Track(source2, None, trackdur*60, beamName="1", fixedOffset=ofst(0.5))

  Configure(ccbptcspnt2)
  killlo()
  undead()

  AutoPeakFocus(source1, configure=False, balance=False, beamName="1")
  numtracks = numtracks-1
```

## B. A menagerie of antenna servo error plots

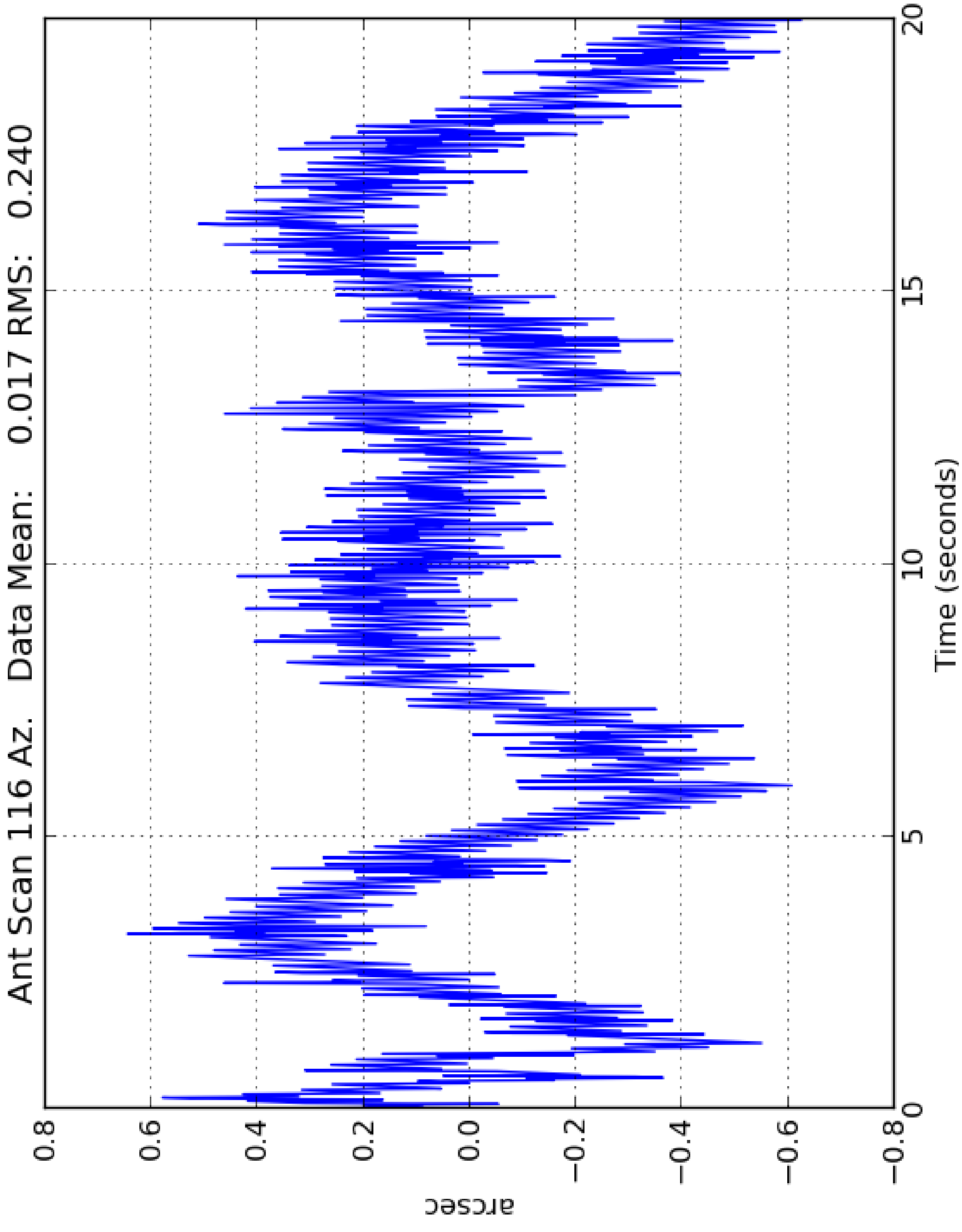


Fig. A1.— Antenna azimuth servo error, scan 116

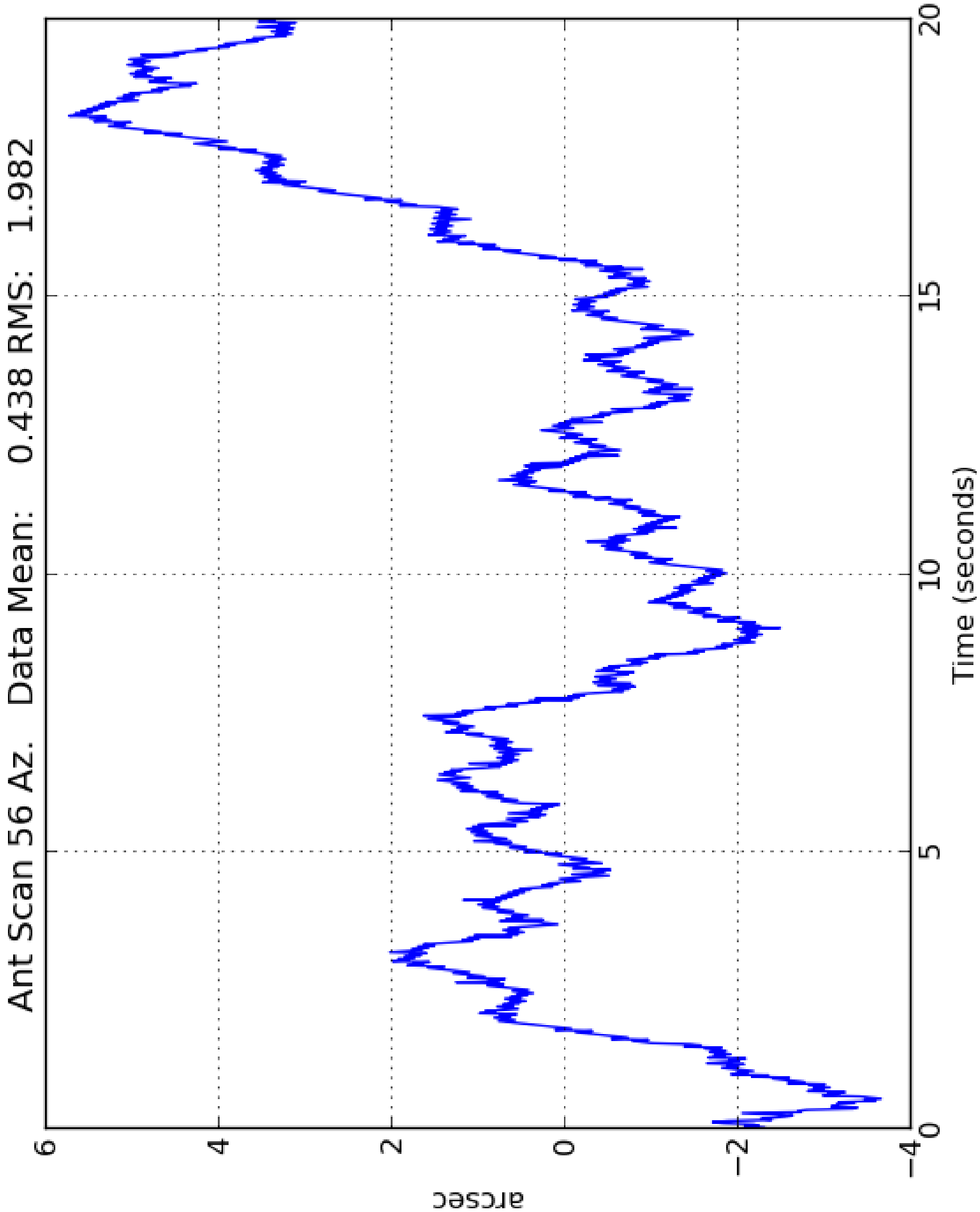


Fig. A2.— Antenna azimuth servo error, scan 56

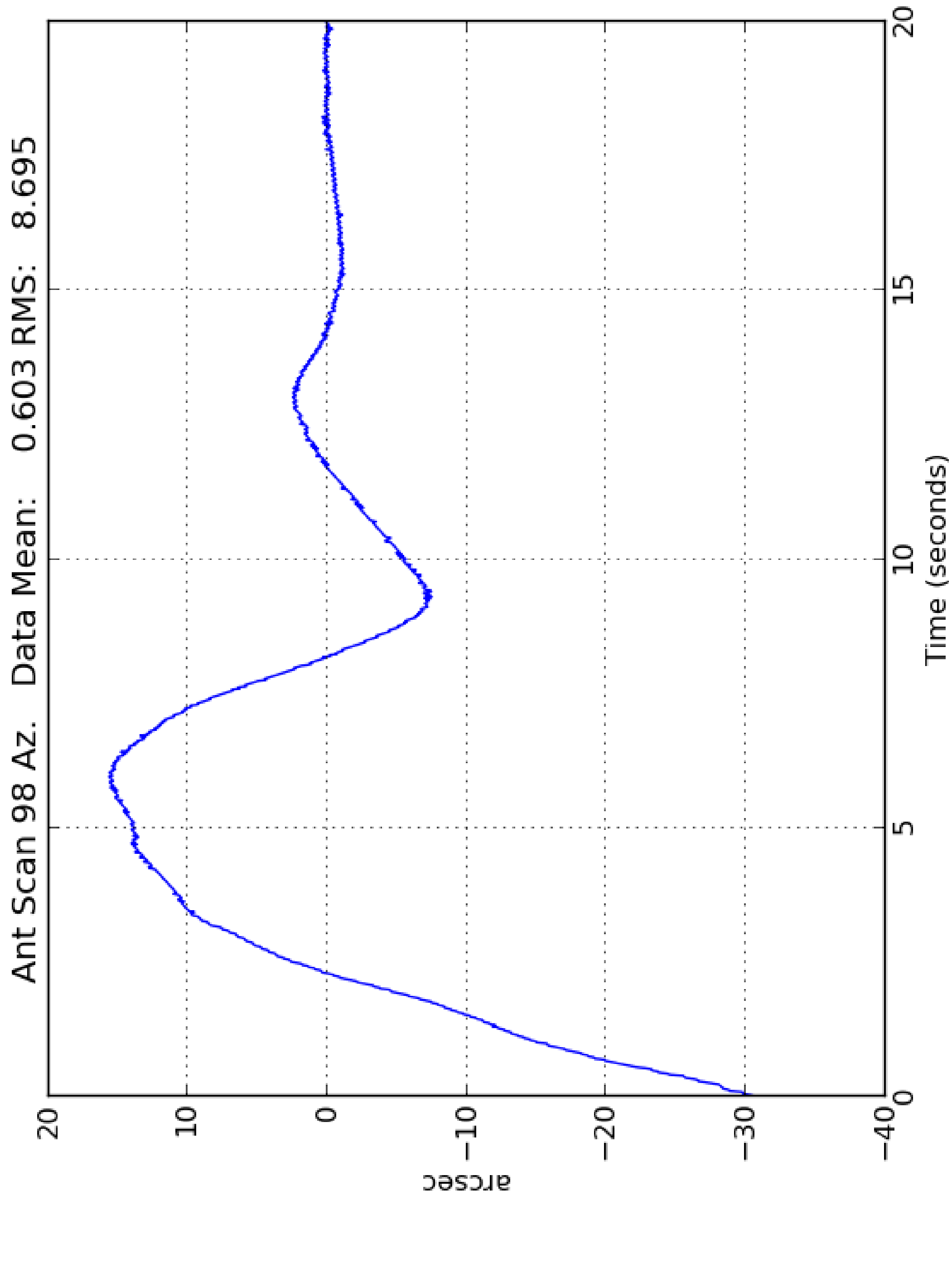


Fig. A3.— Antenna azimuth servo error, scan 98

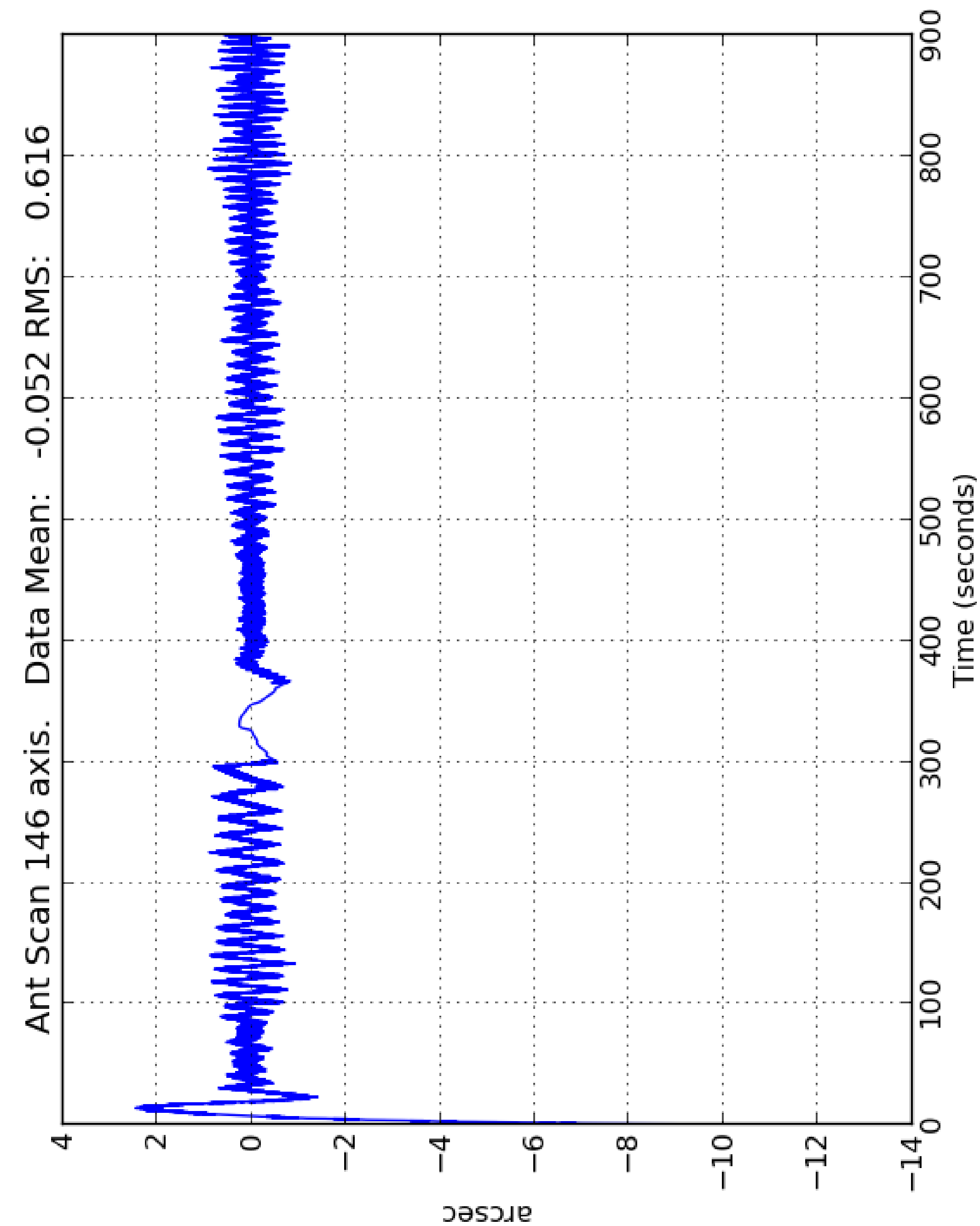


Fig. A4.— Antenna azimuth servo error, scan 146

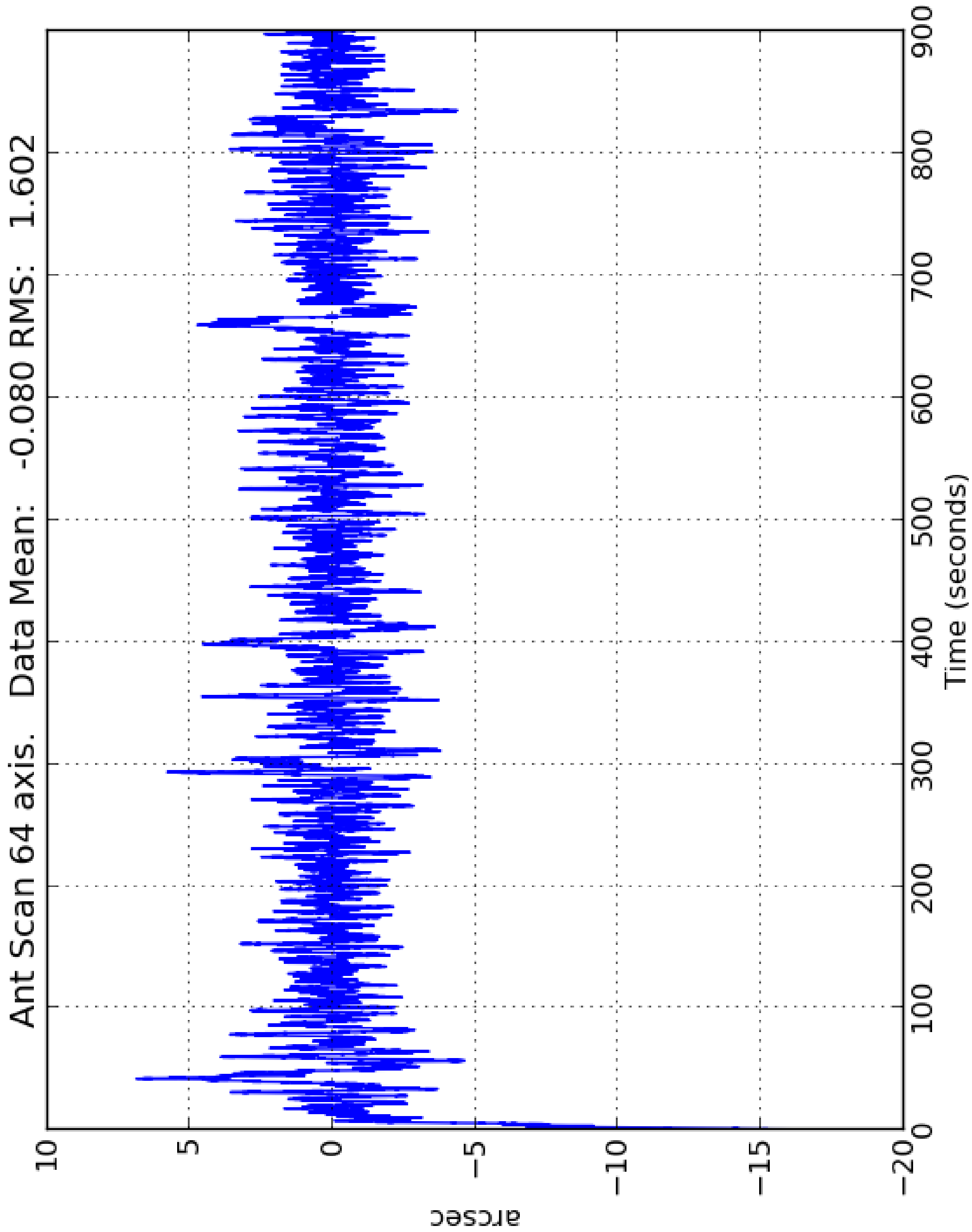


Fig. A5.— Antenna azimuth servo error, scan 64

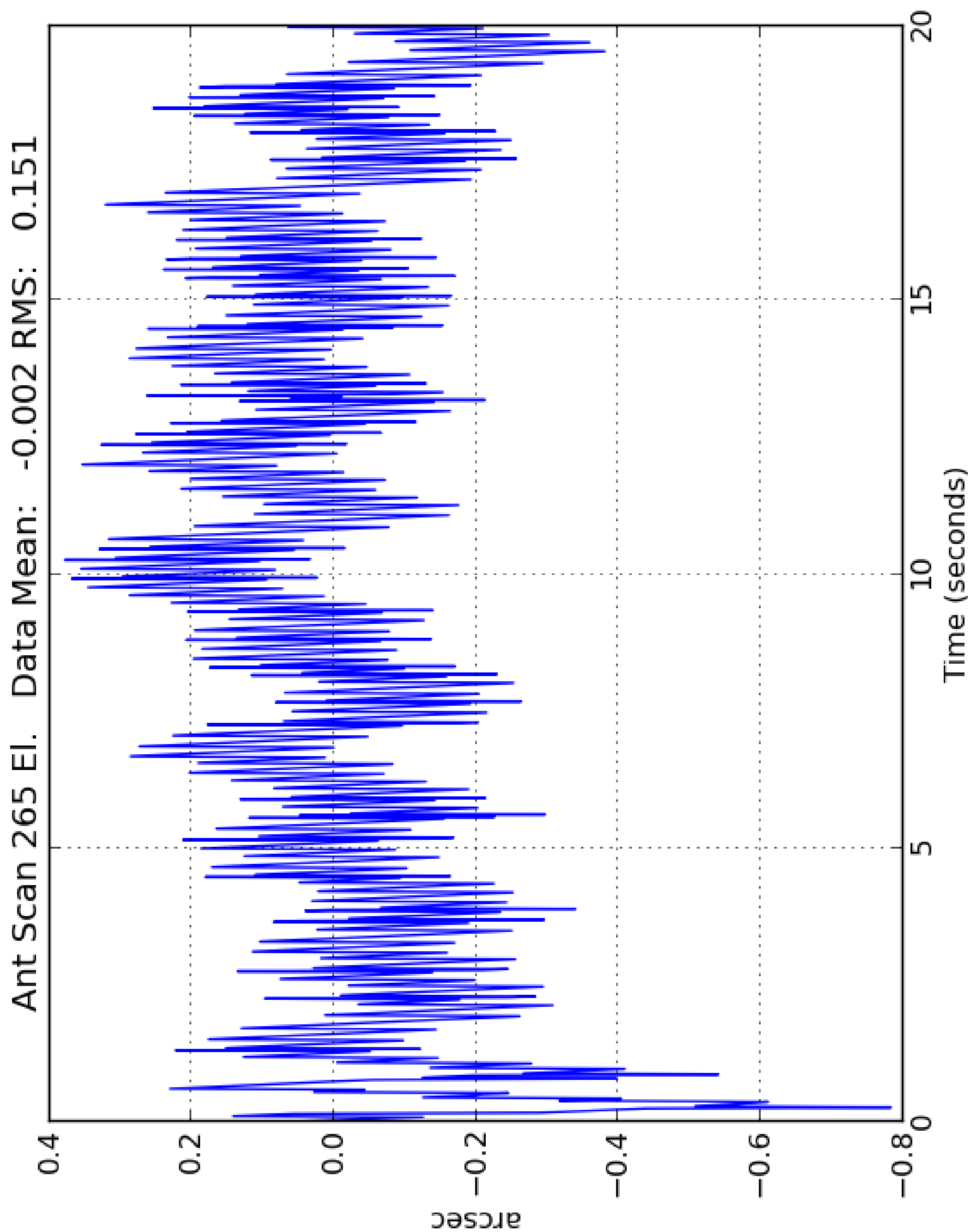


Fig. A6.— Antenna elevation servo error, scan 265

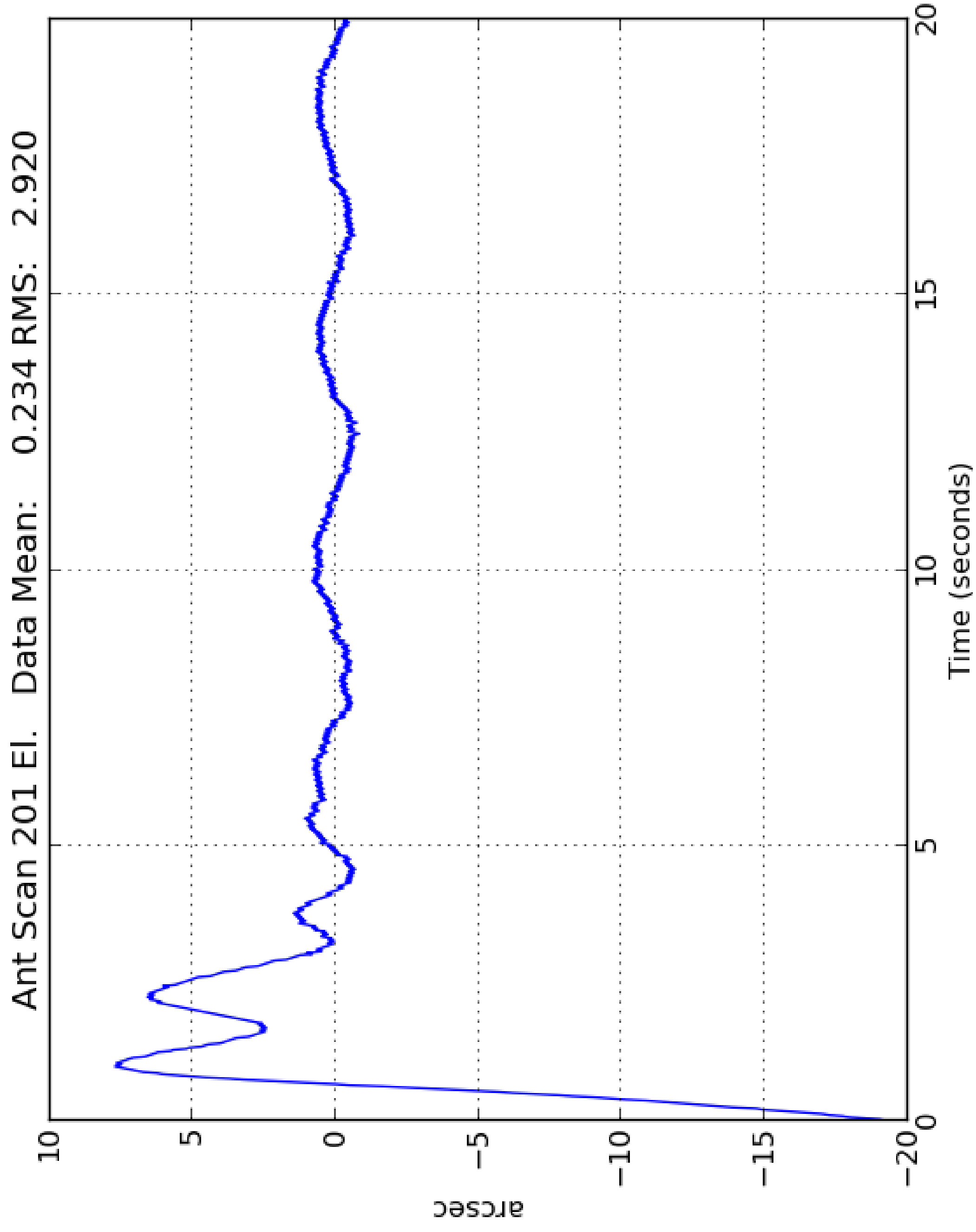


Fig. A7.— Antenna elevation servo error, scan 201

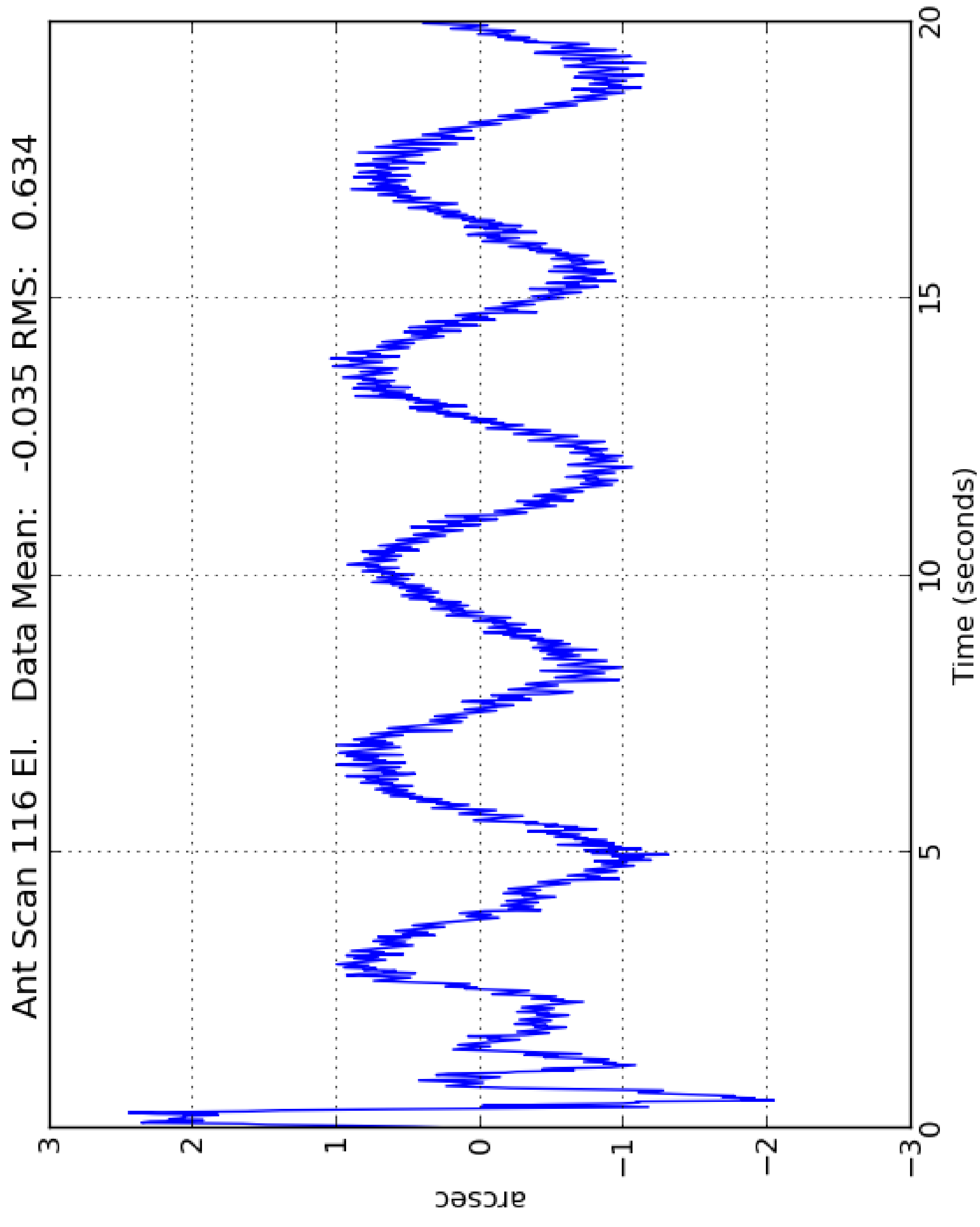


Fig. A8.— Antenna elevation servo error, scan 116

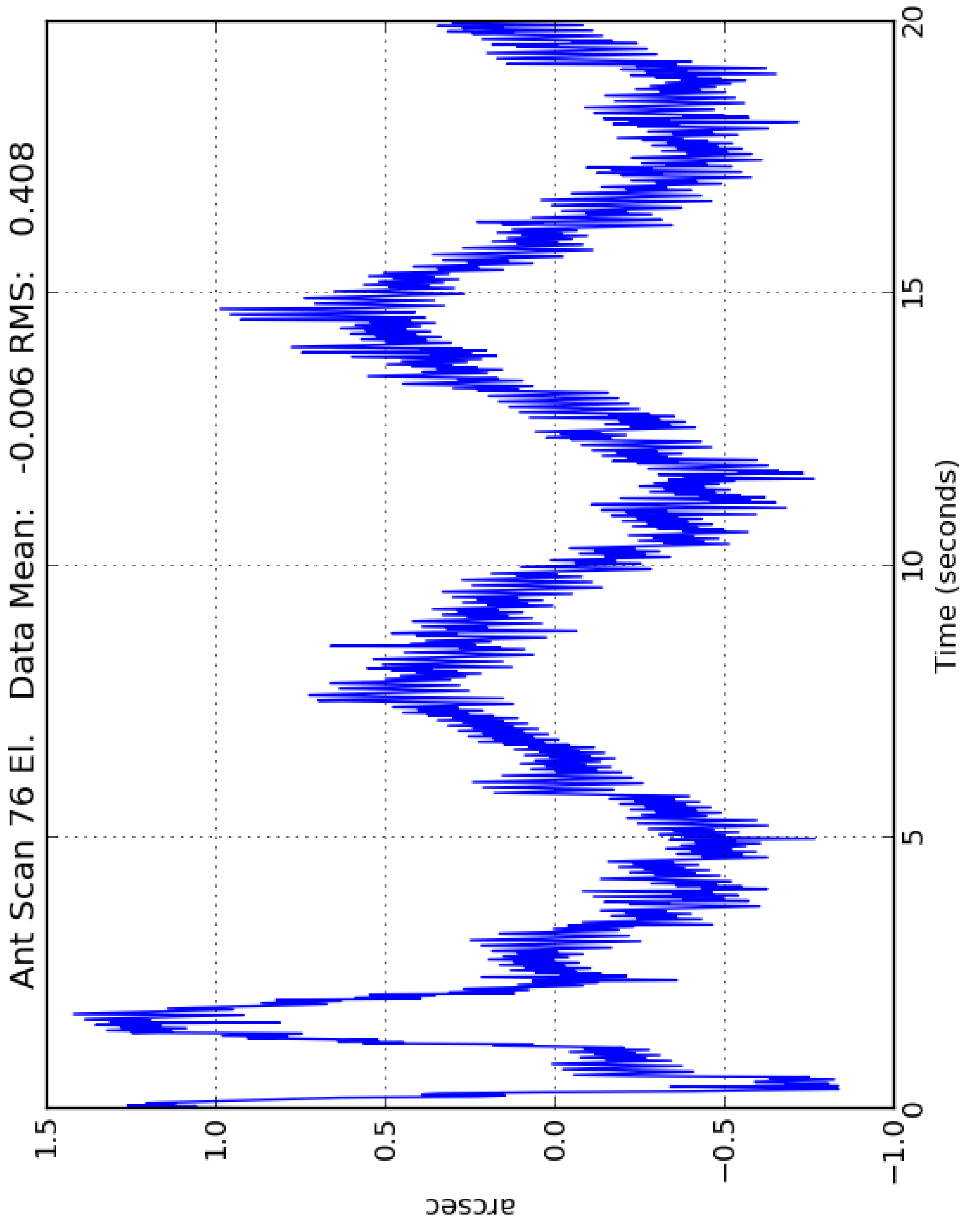


Fig. A9.— Antenna elevation servo error, scan 176

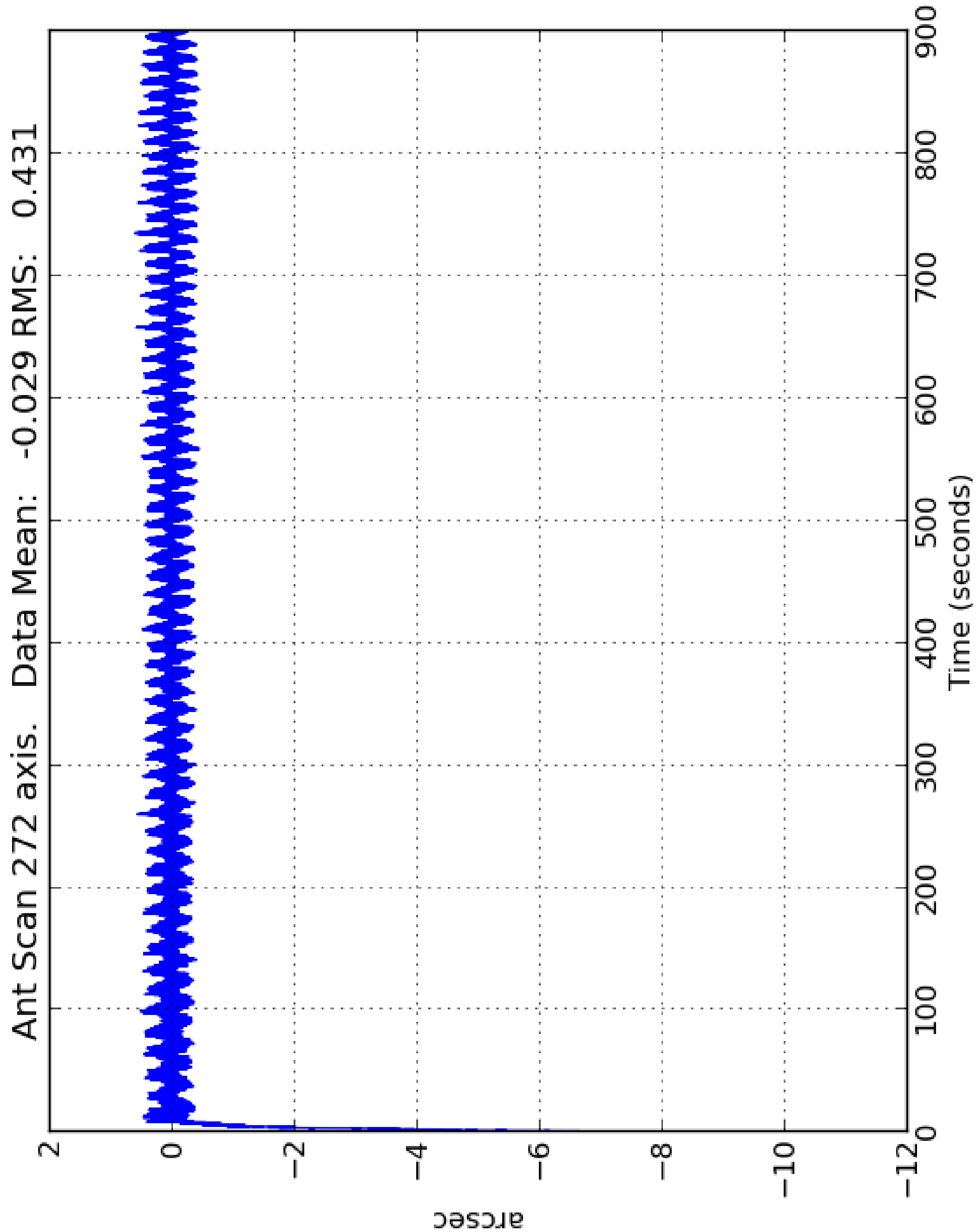


Fig. A10.— Antenna elevation servo error, scan 272

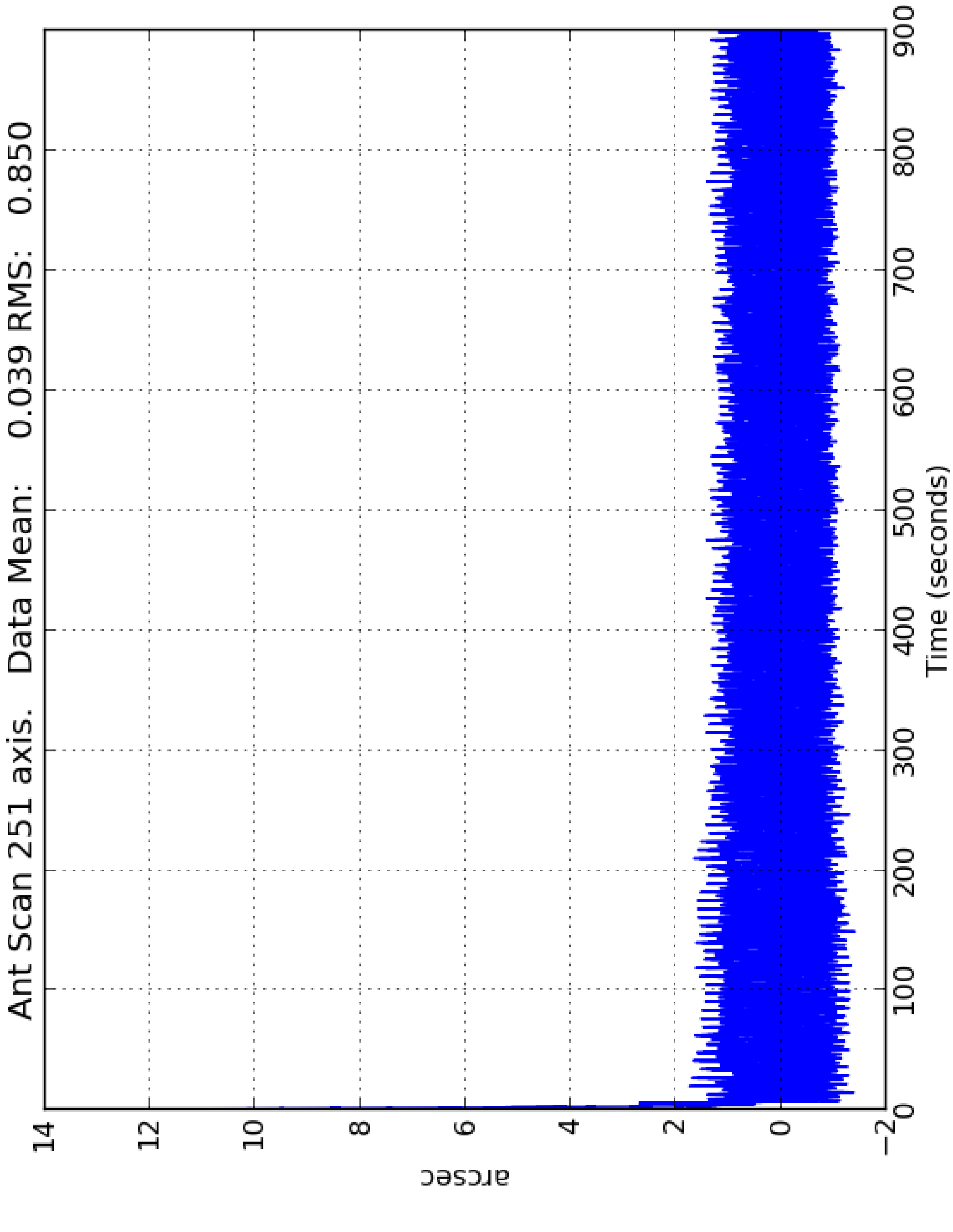


Fig. A11.— Antenna elevation servo error, scan 251

## C. Quadrant Detector Plots

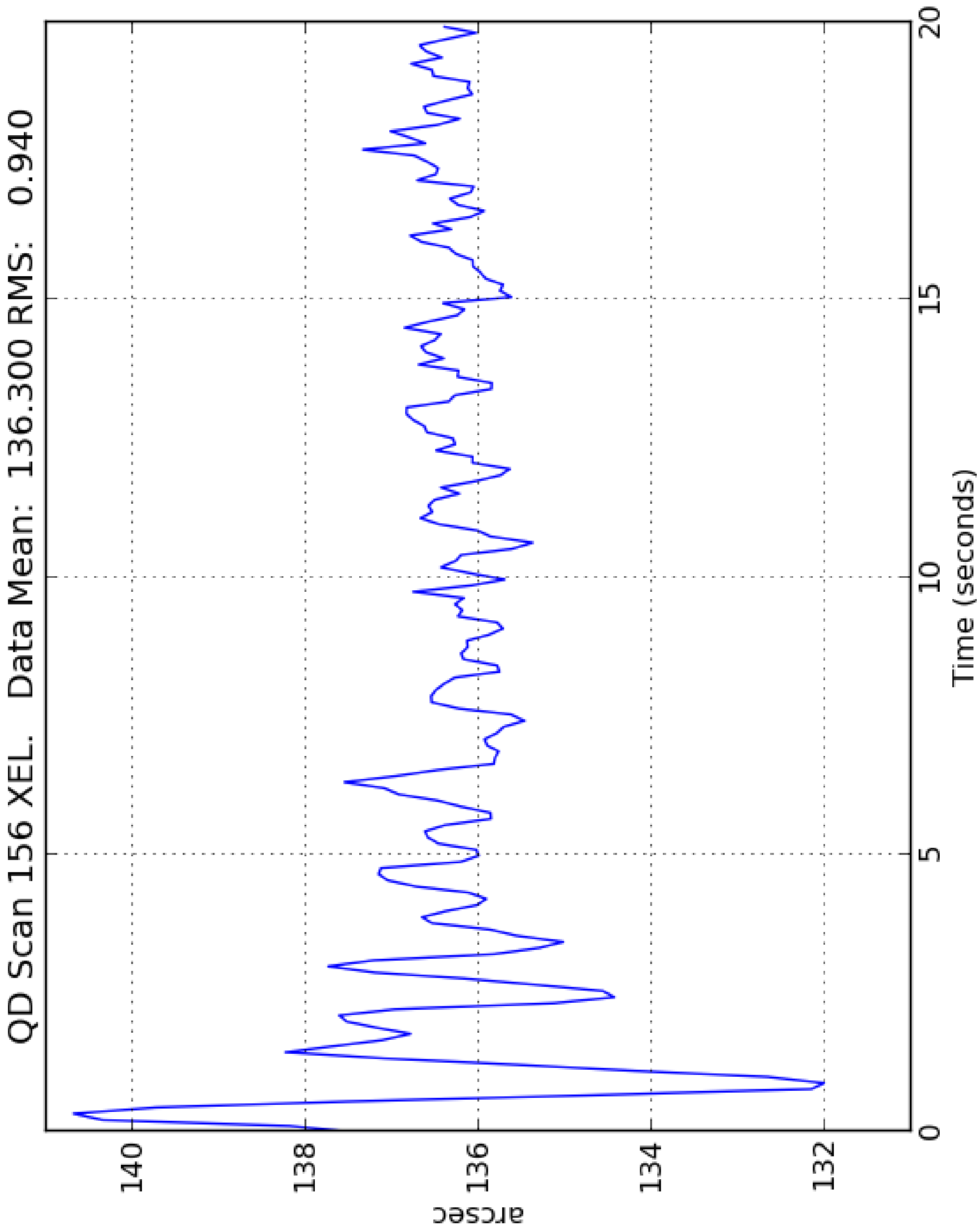


Fig. B1.— Quadrant detector cross-elevation output, scan 156

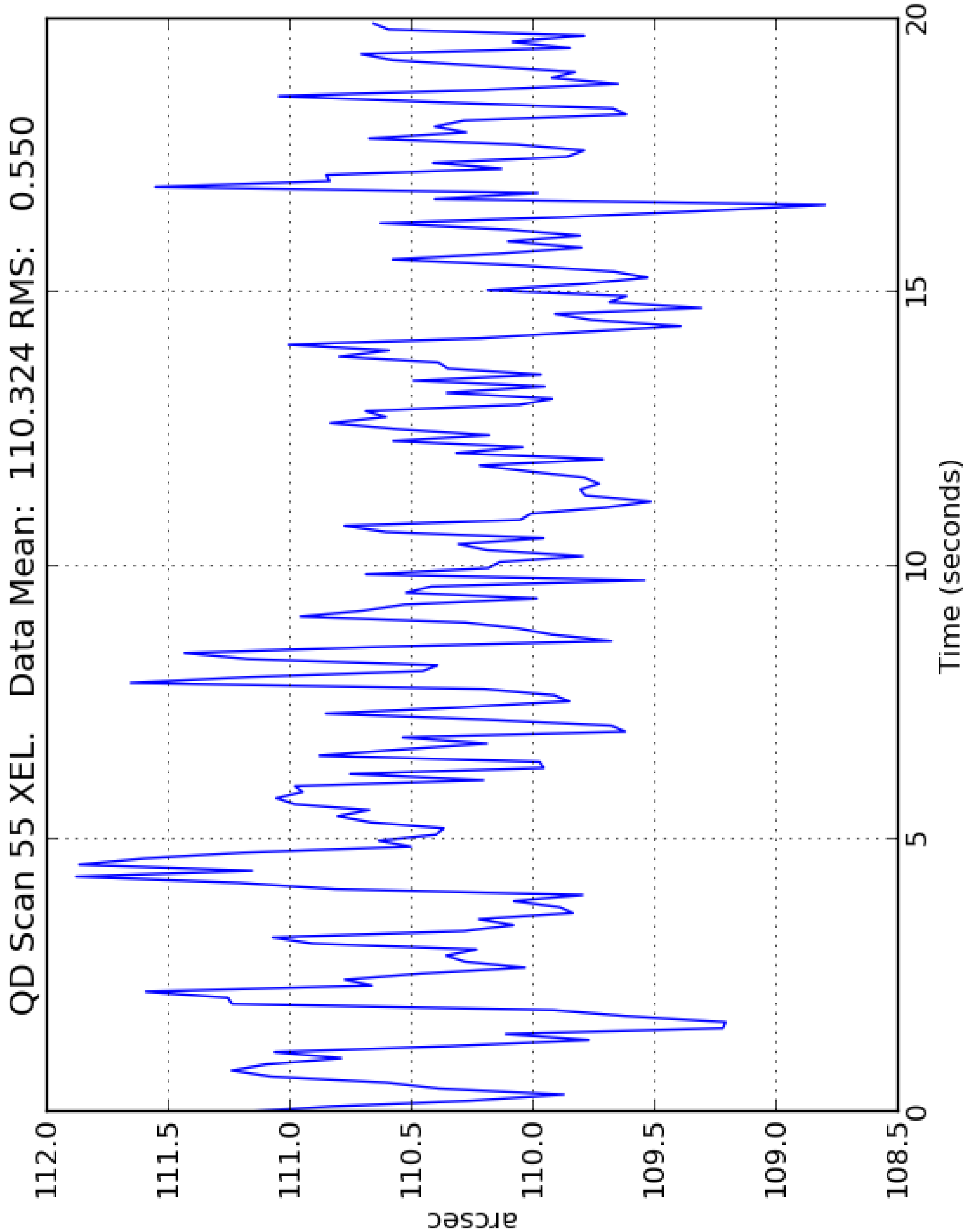


Fig. B2.— Quadrant detector cross-elevation output, scan 55

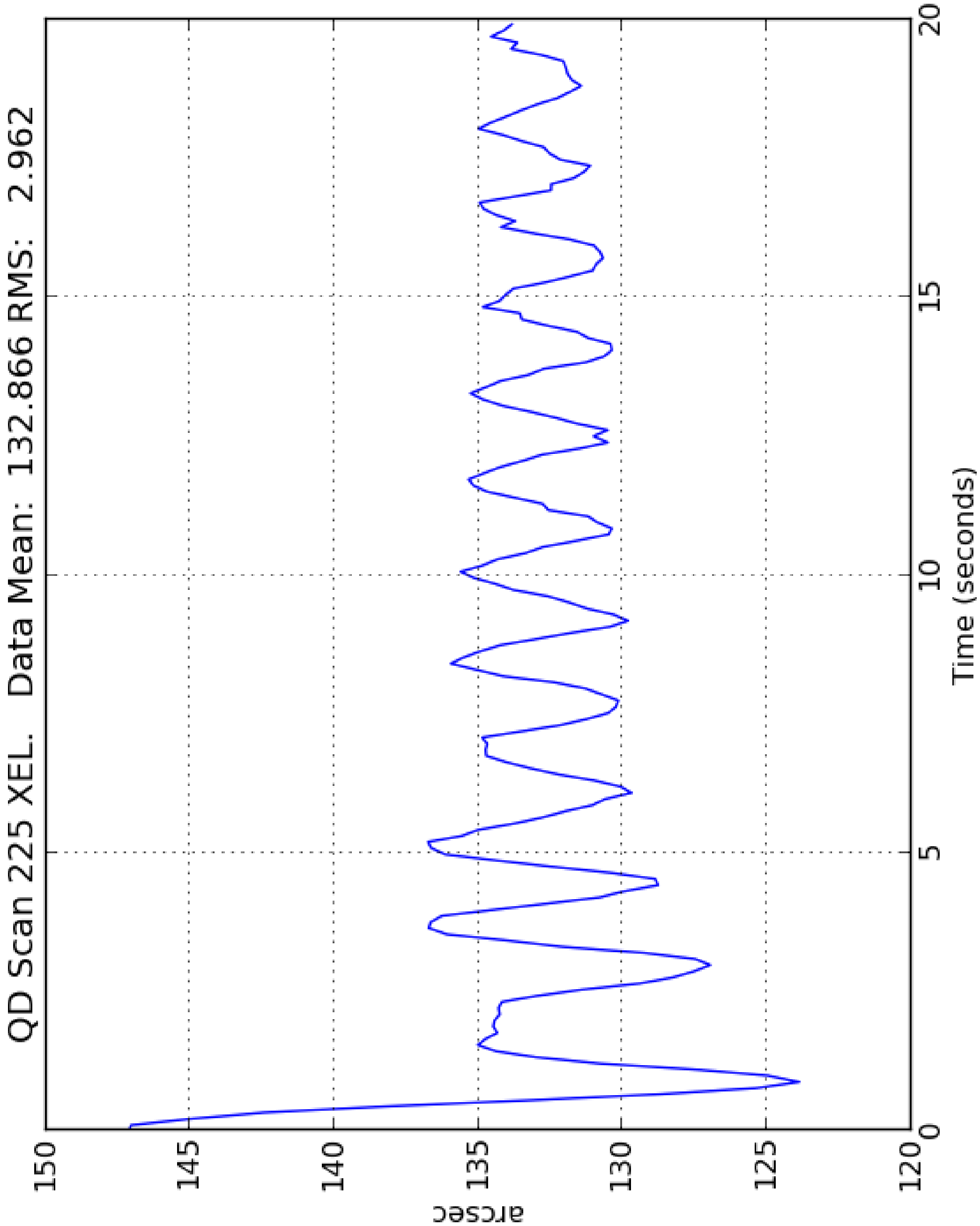


Fig. B3.— Quadrant detector cross-elevation output, scan 225

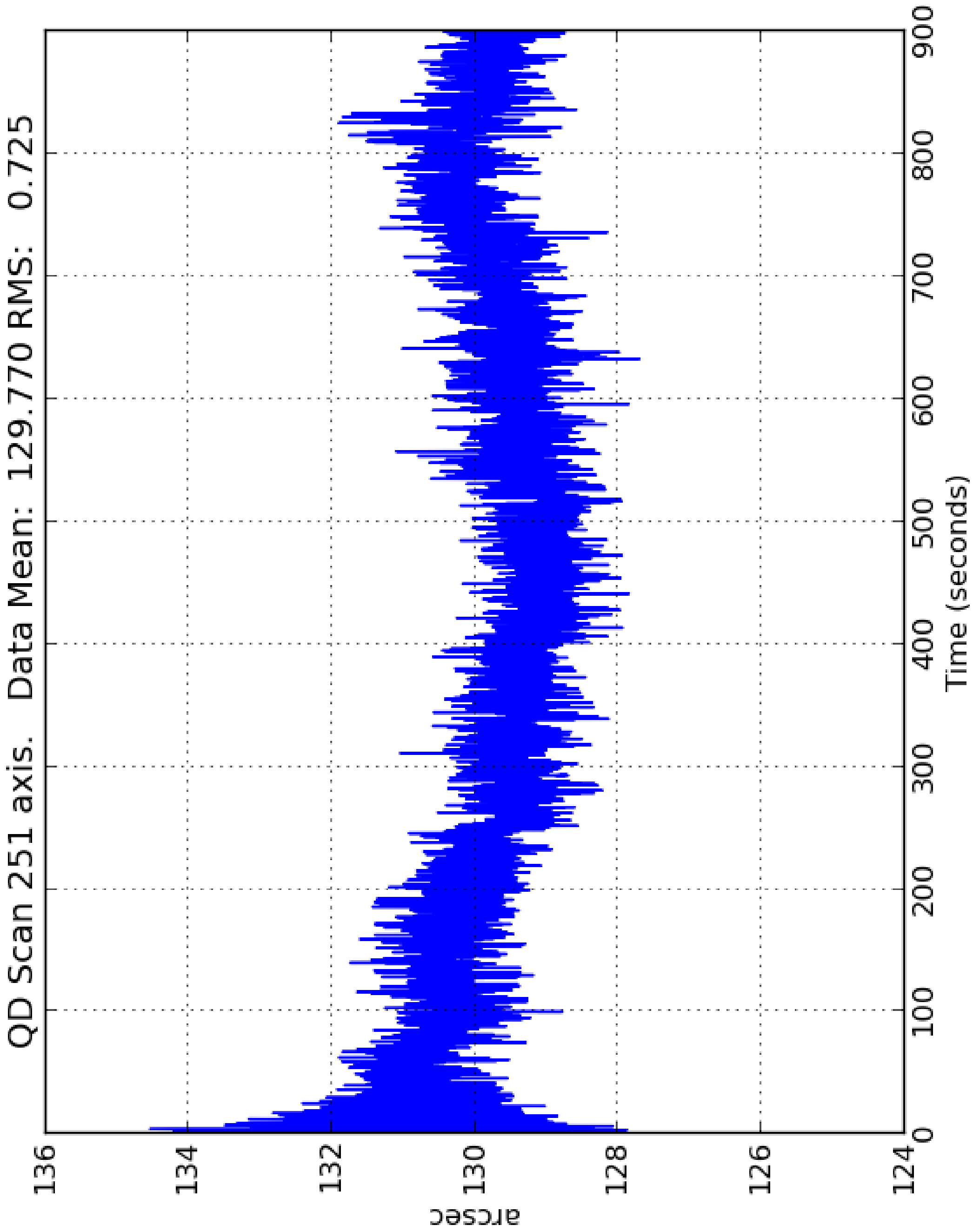


Fig. B4.— Quadrant detector cross-elevation output, scan 251

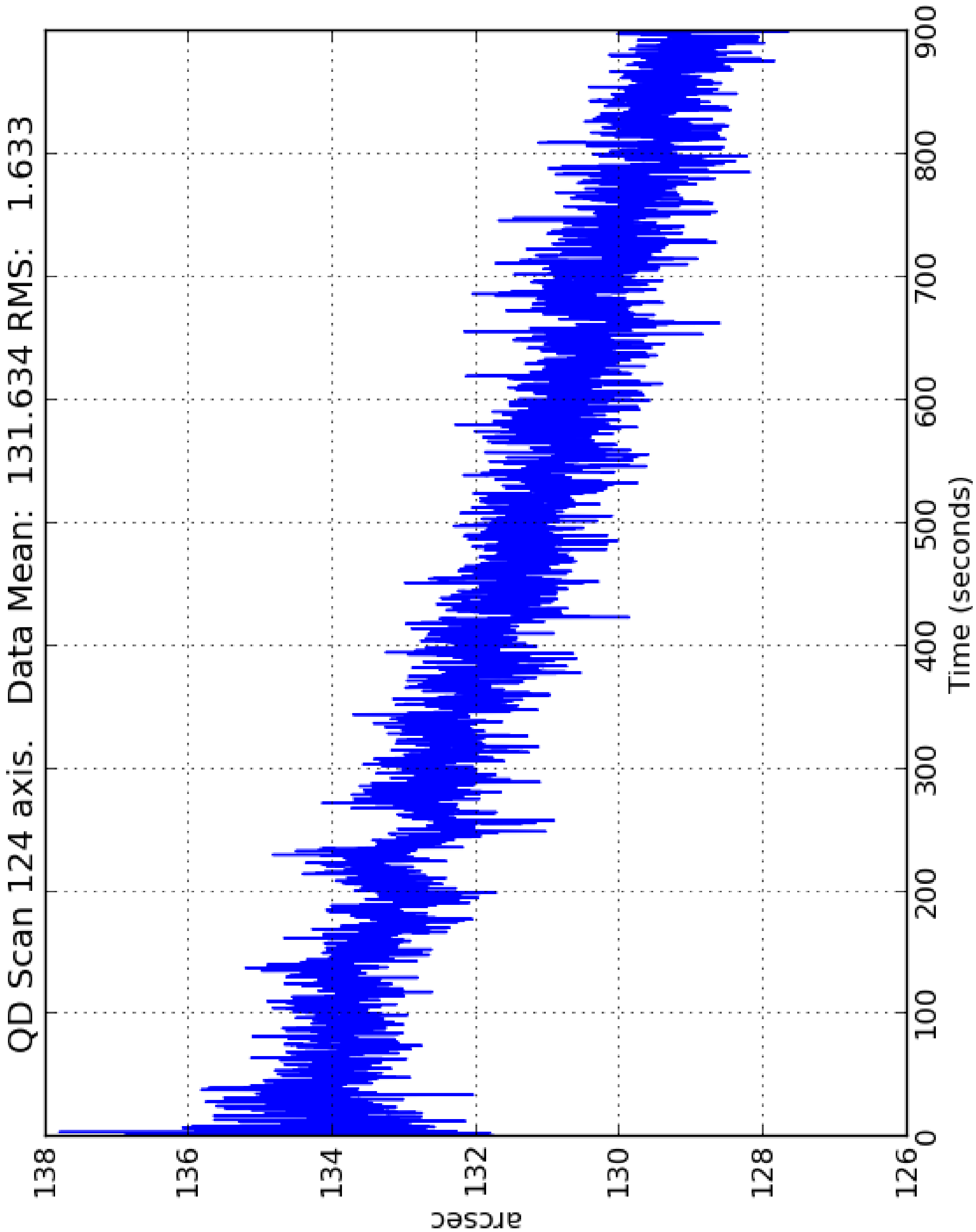


Fig. B5.— Quadrant detector cross-elevation output, scan 124

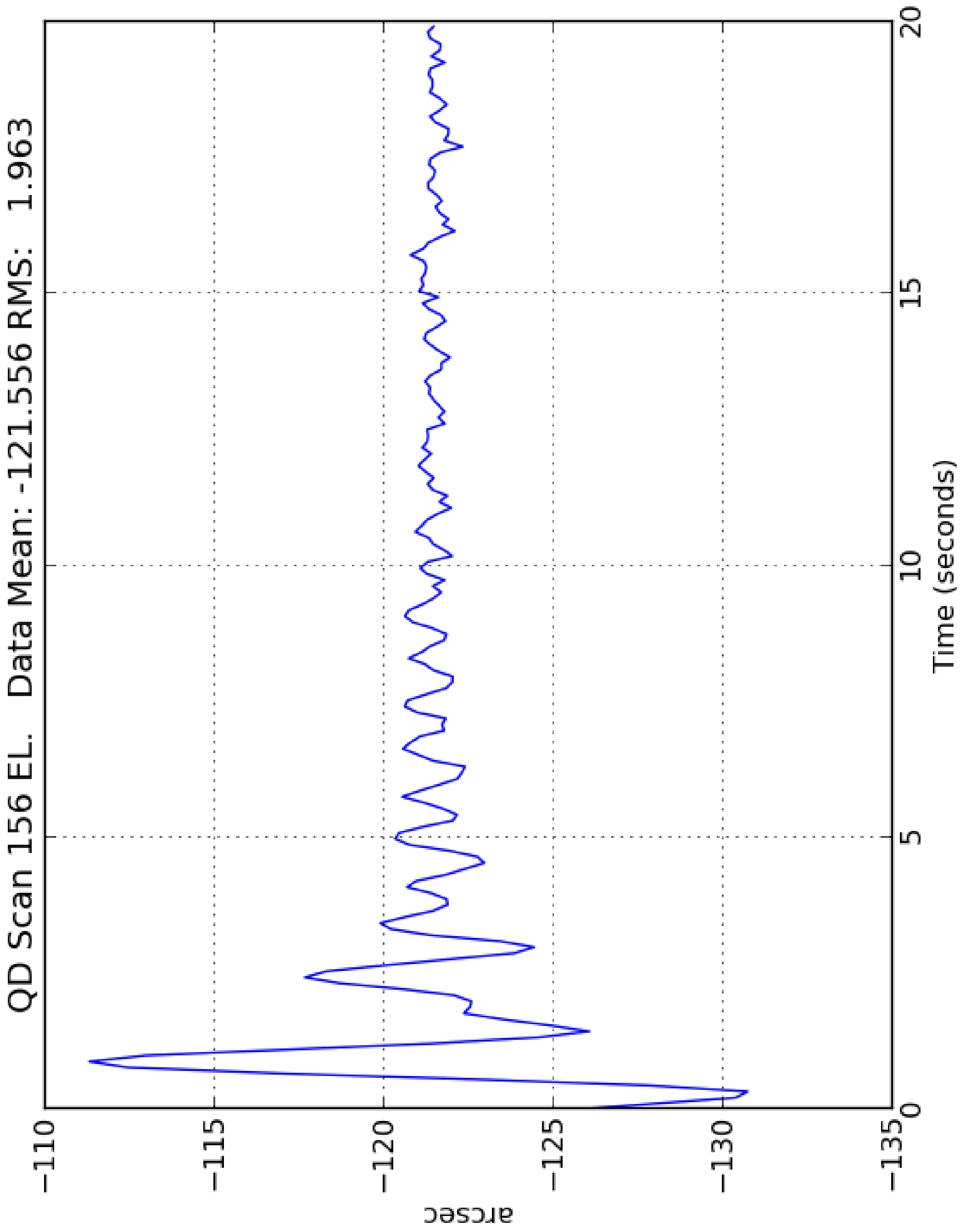


Fig. B6.— Quadrant detector elevation output, scan 156

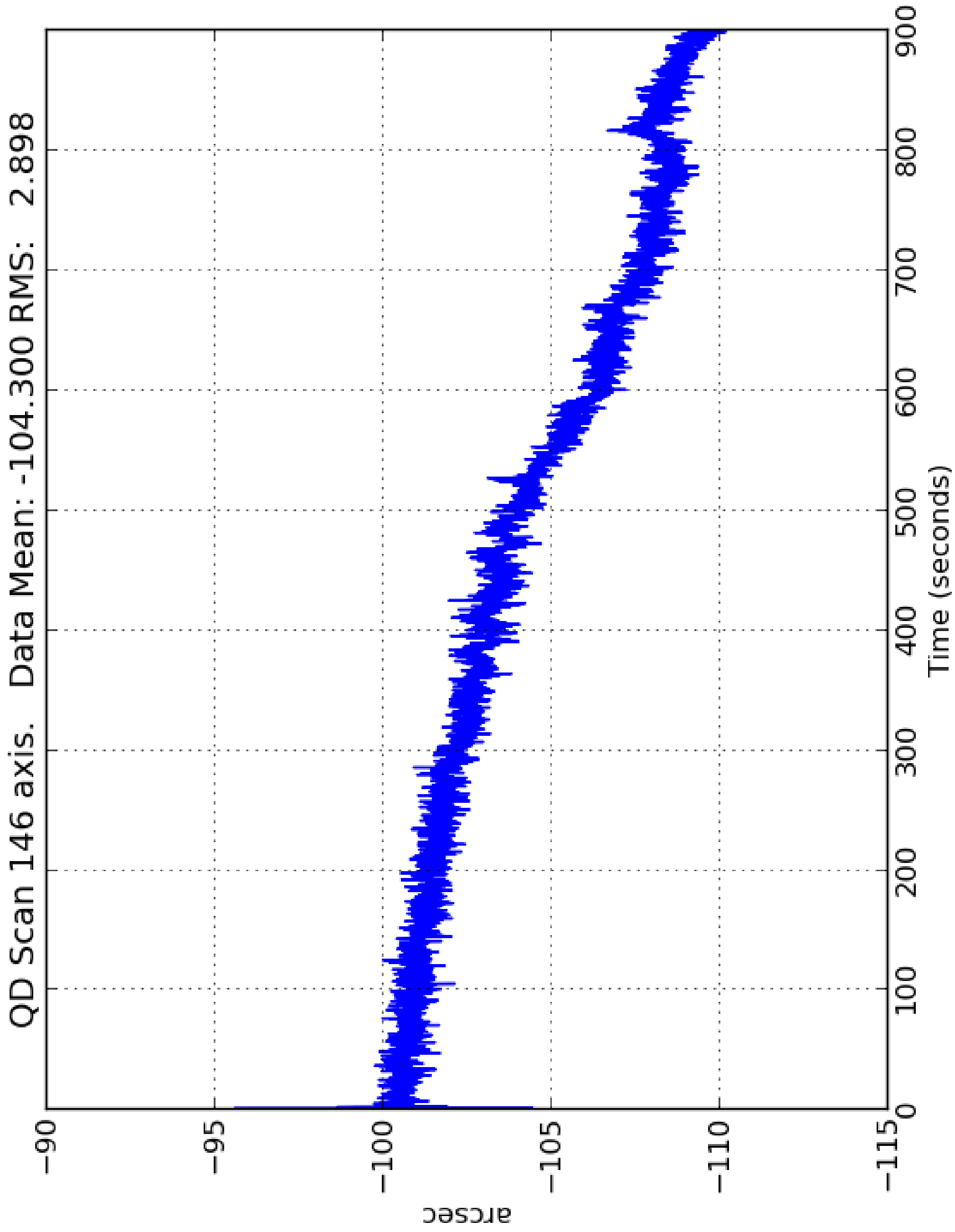


Fig. B7.— Quadrant detector elevation output, scan 146

## D. Offset Pointing Data

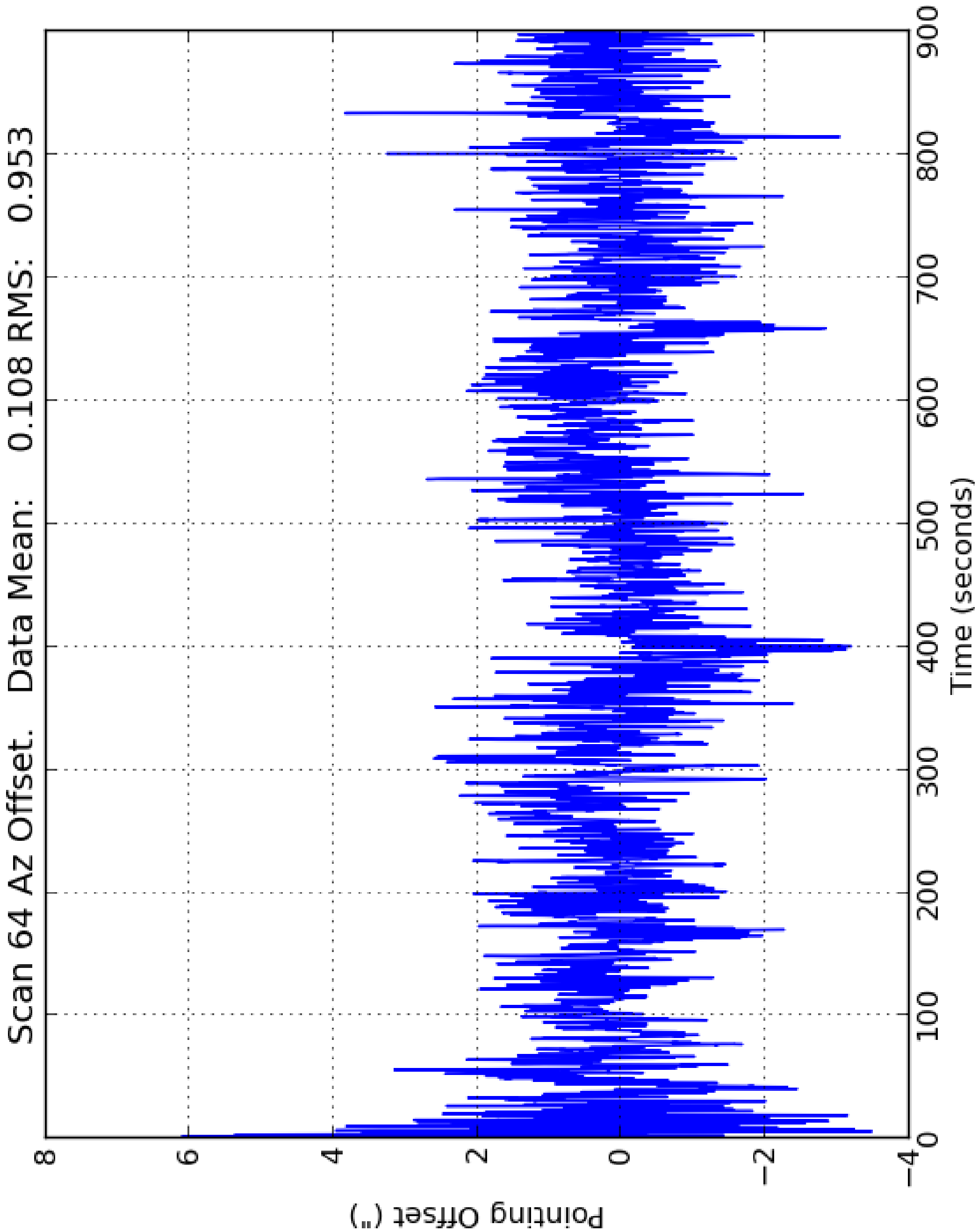


Fig. C1.— Half-power tracking data for scan 64

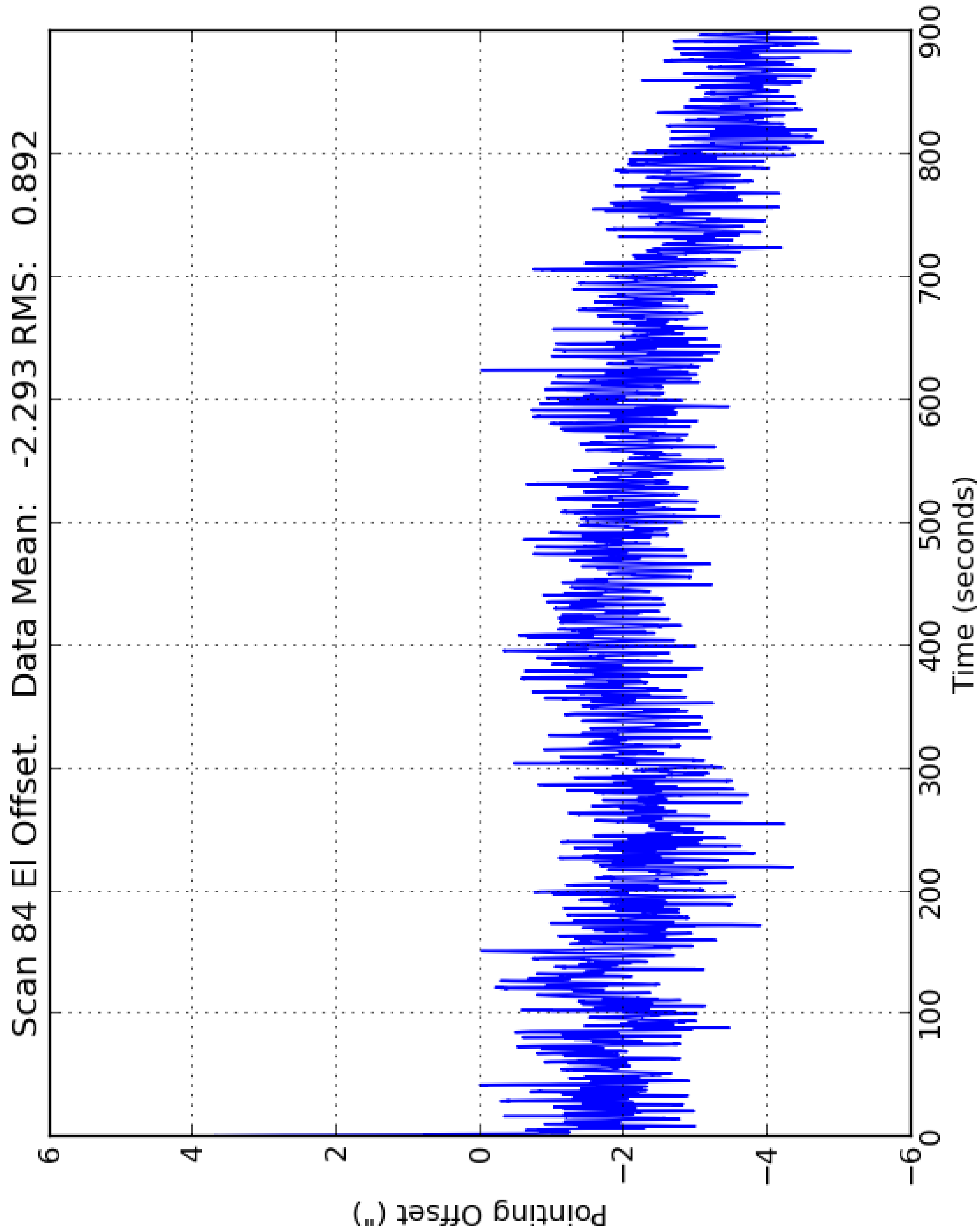


Fig. C2.— Half-power tracking data for scan 84

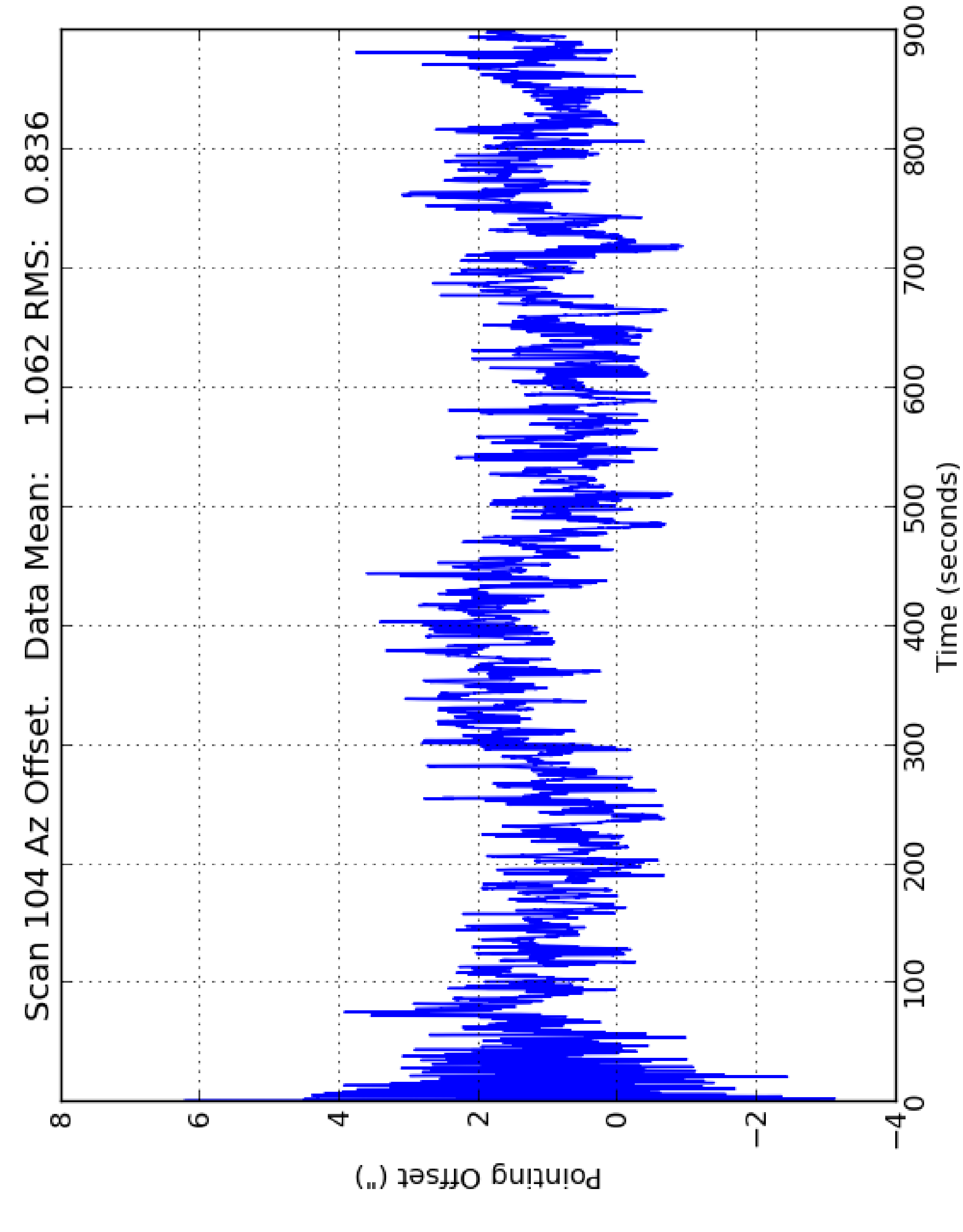


Fig. C3.— Half-power tracking data for scan 104

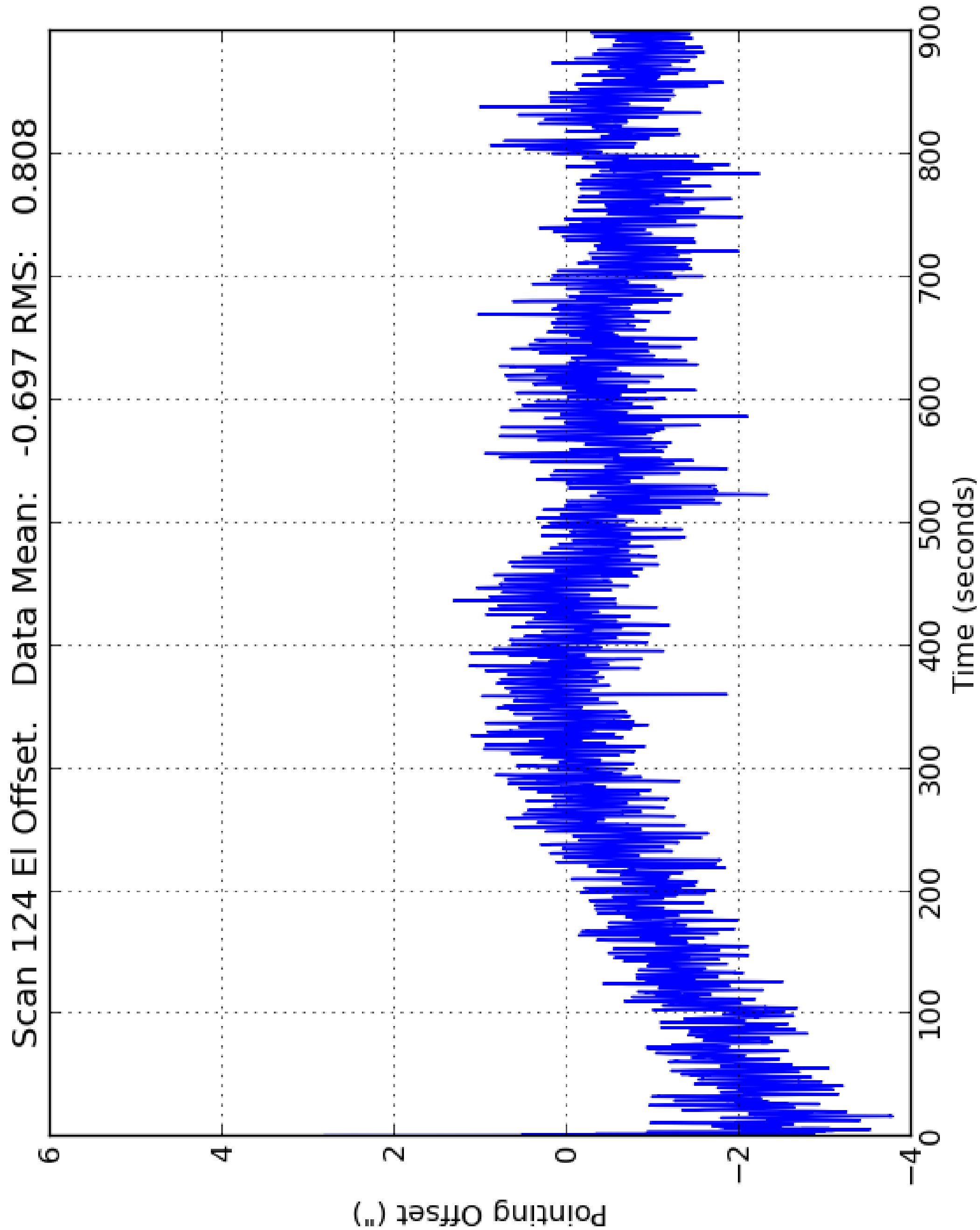


Fig. C4.— Half-power tracking data for scan 124

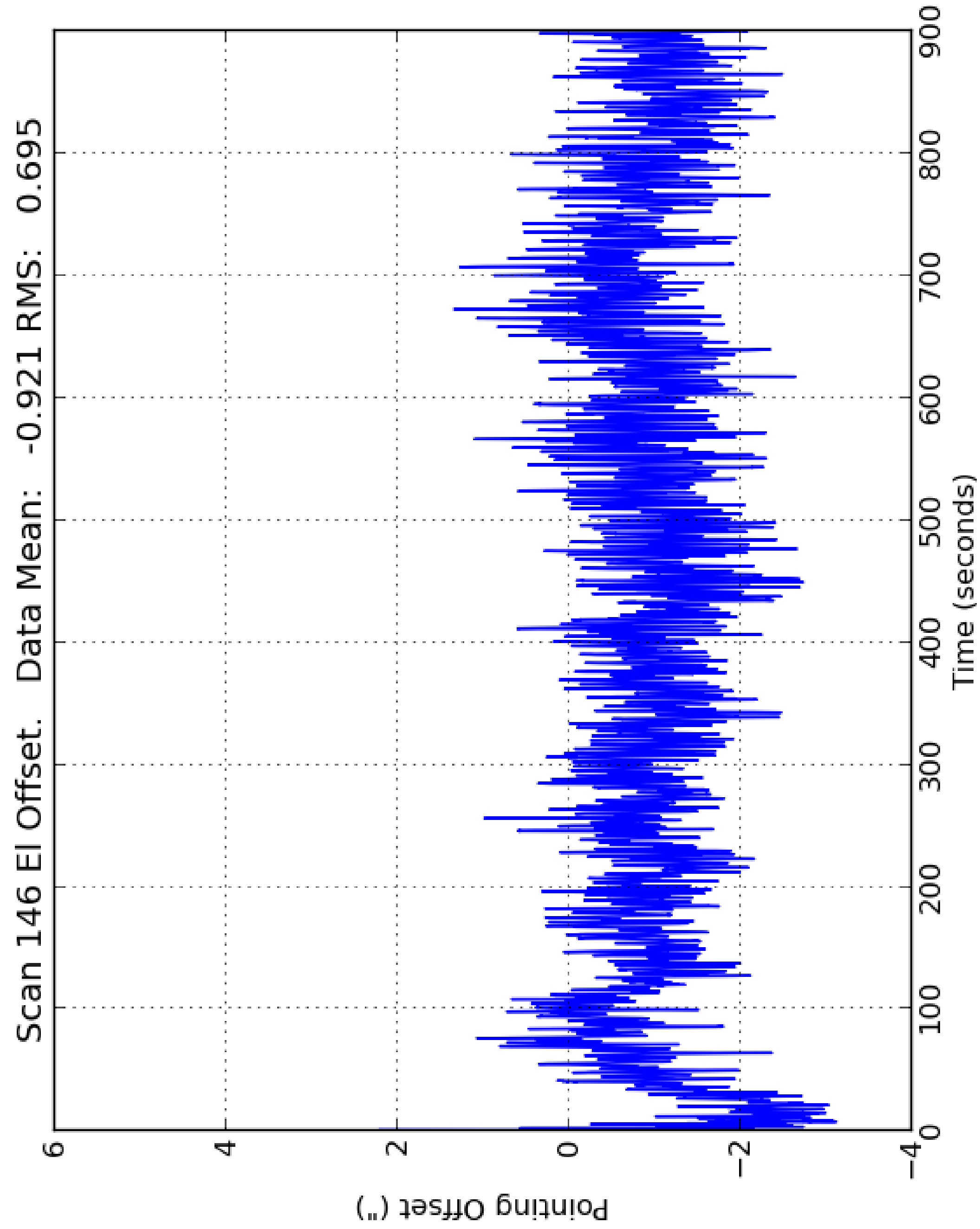


Fig. C5.— Half-power tracking data for scan 146

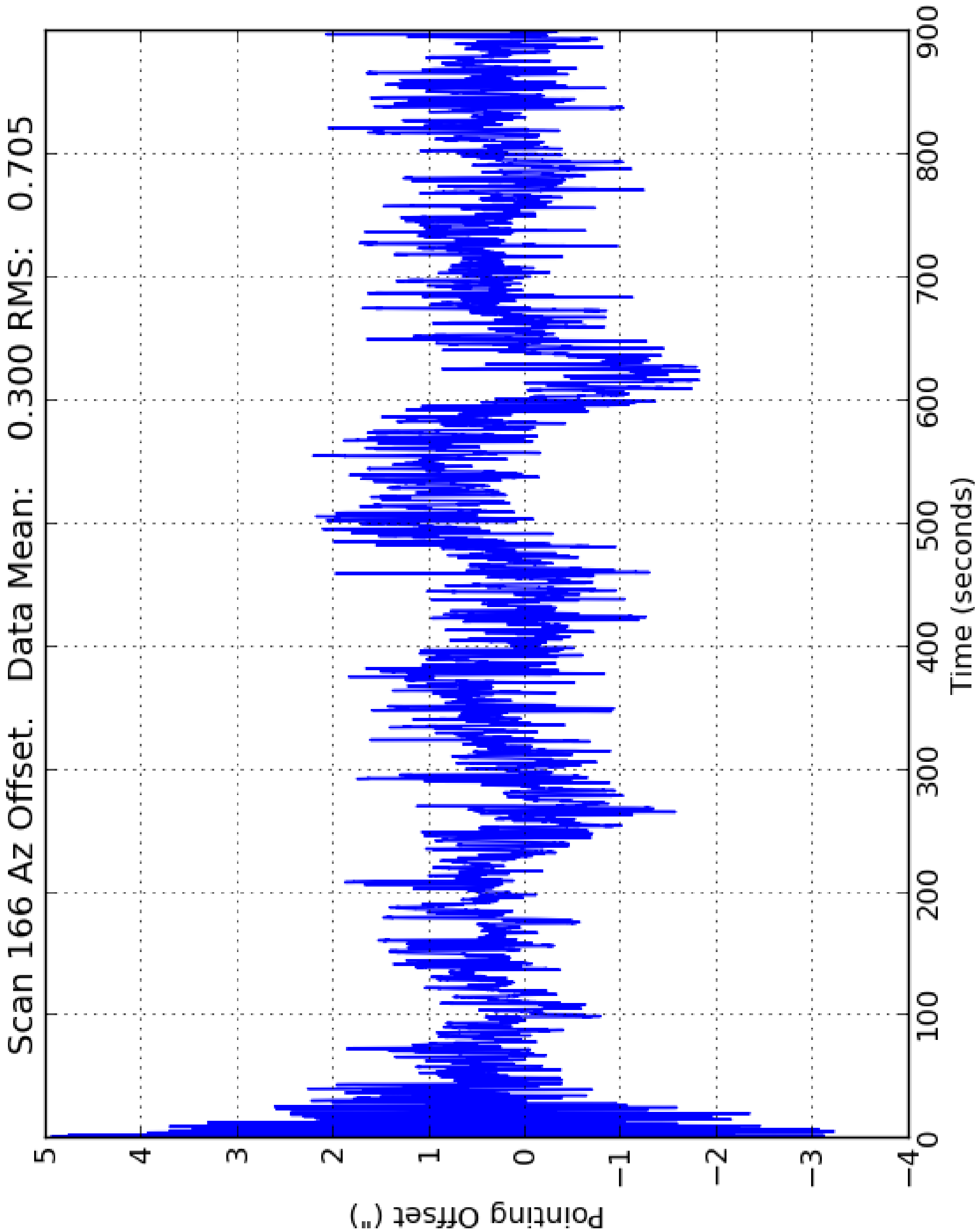


Fig. C6.— Half-power tracking data for scan 166

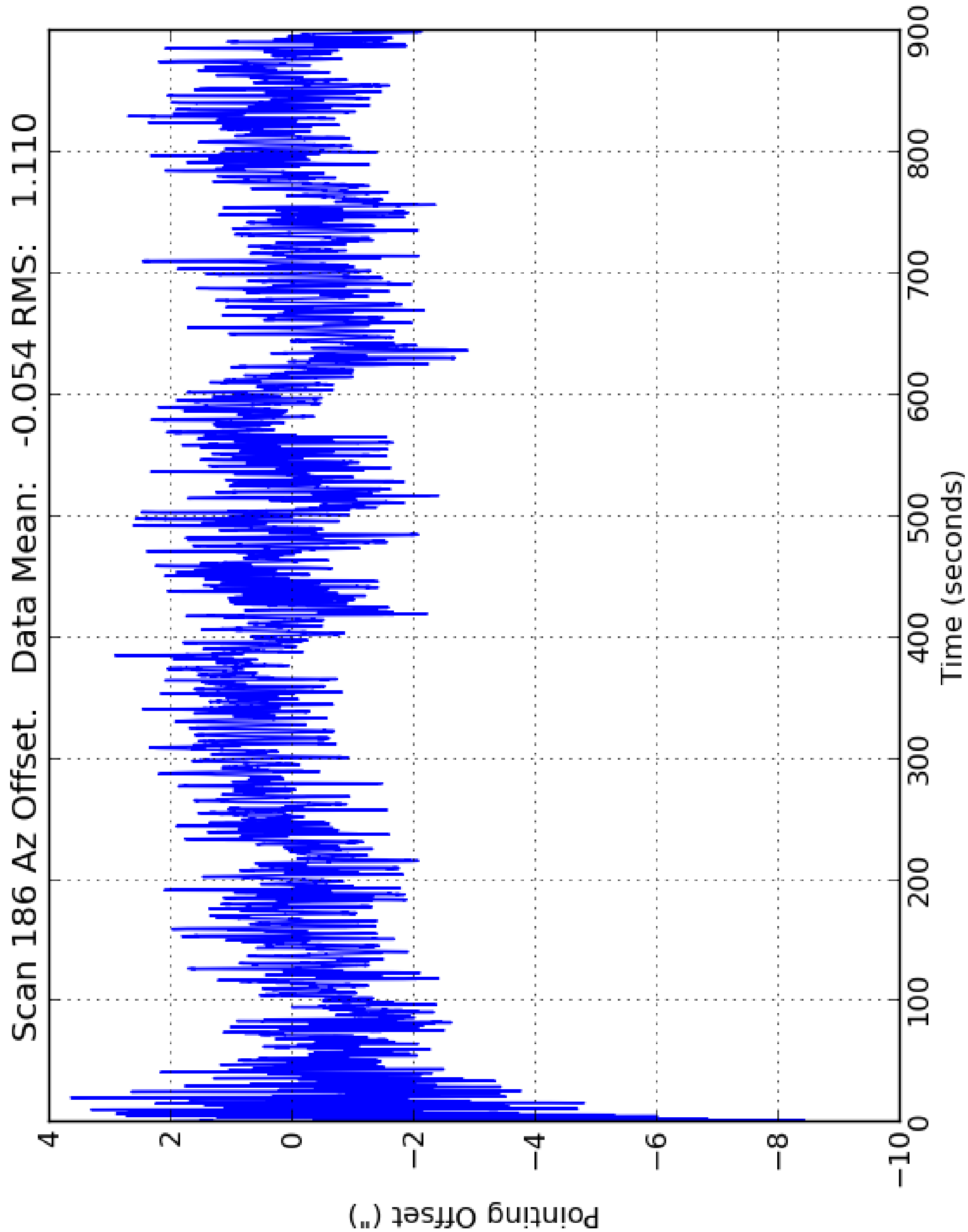


Fig. C7.— Half-power tracking data for scan 186

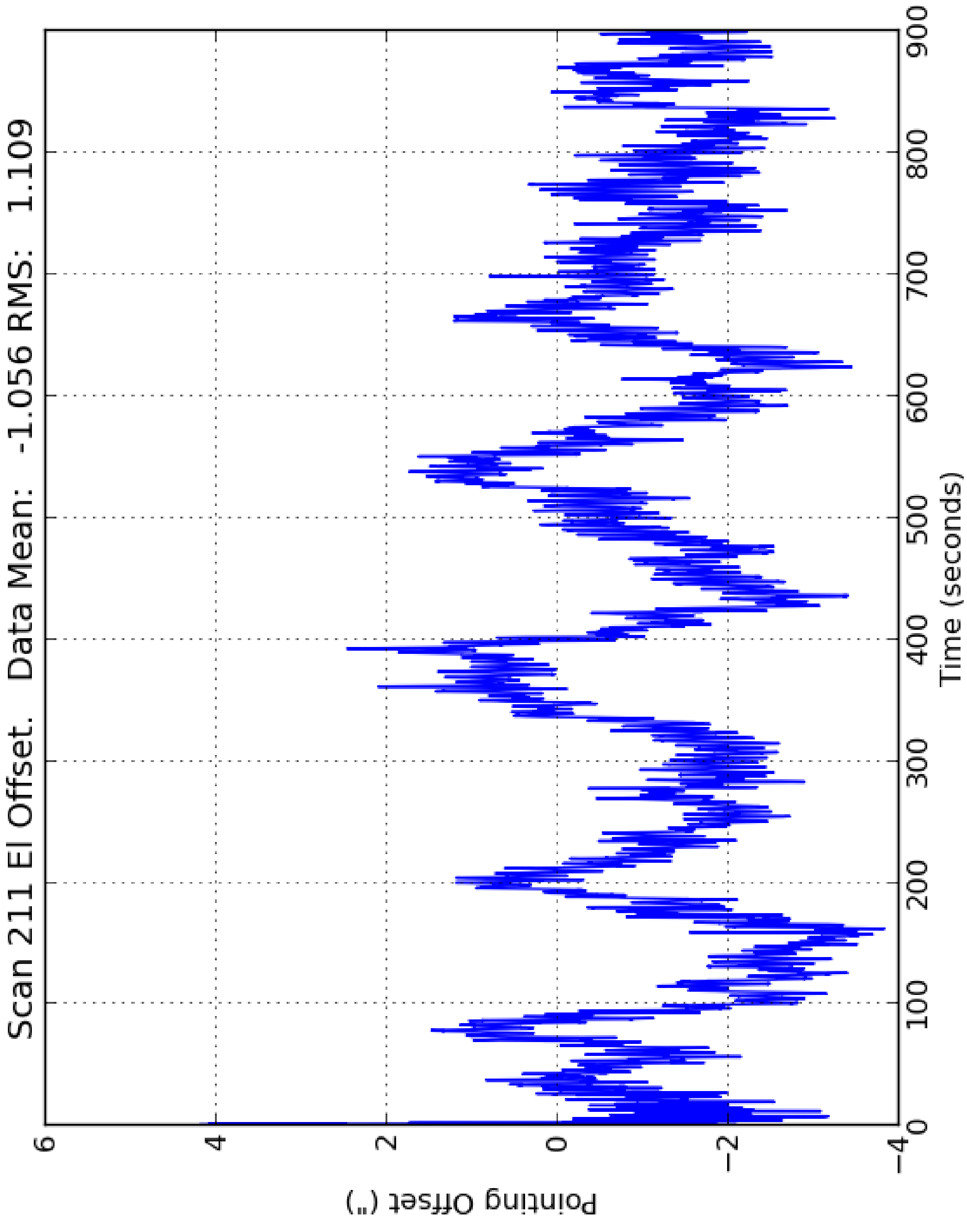


Fig. C8.— Half-power tracking data for scan 211

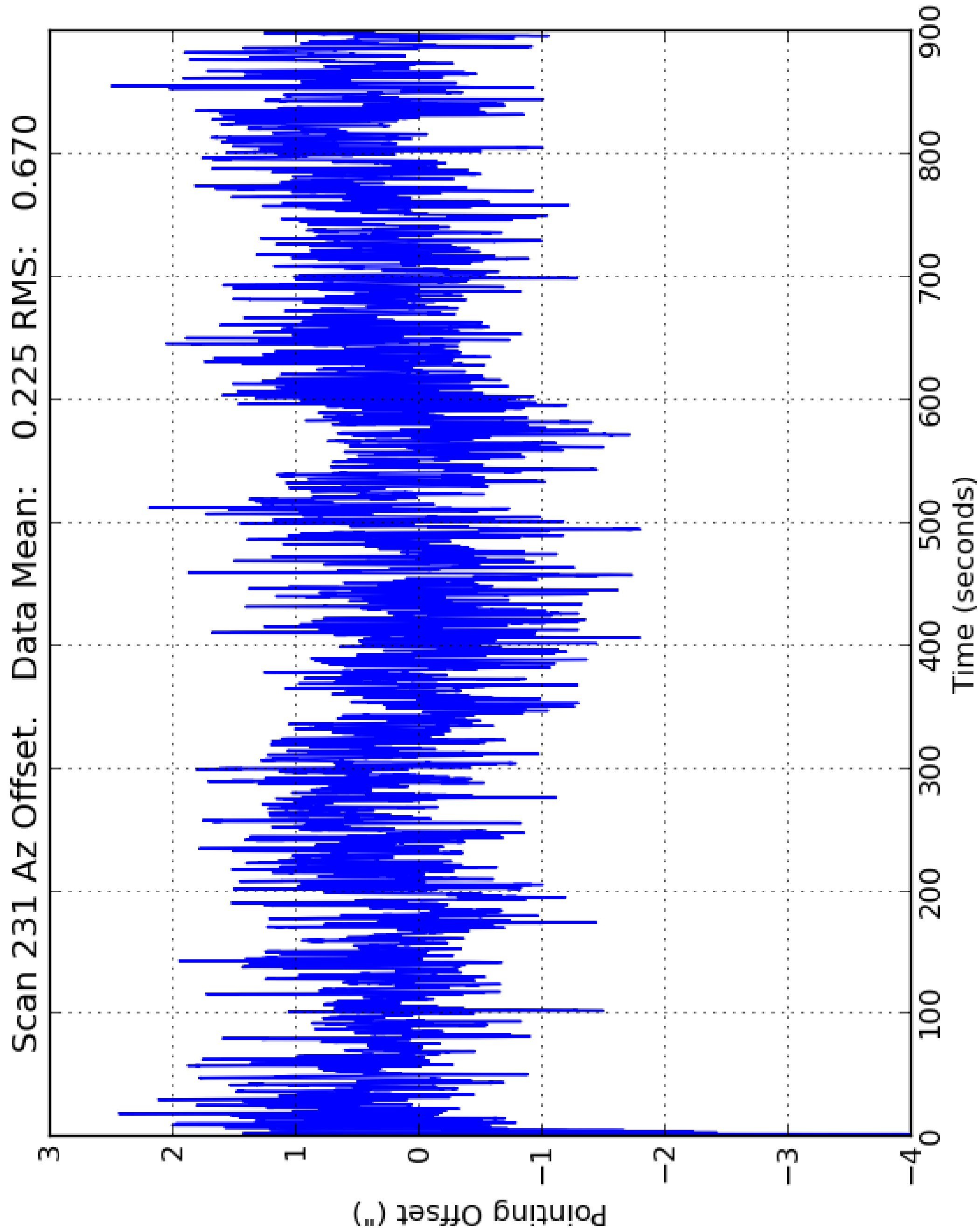


Fig. C9.— Half-power tracking data for scan 231

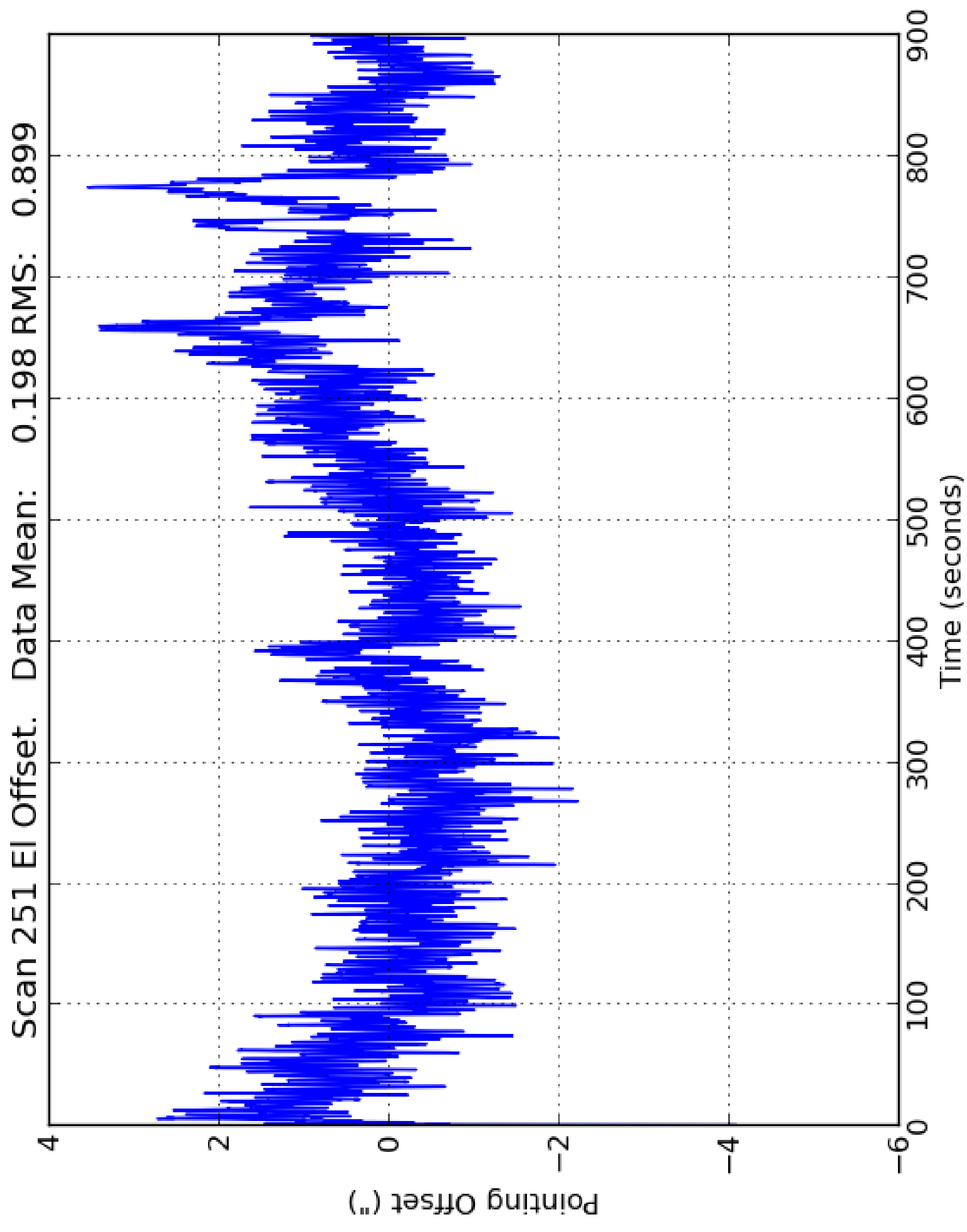


Fig. C10.— Half-power tracking data for scan 251

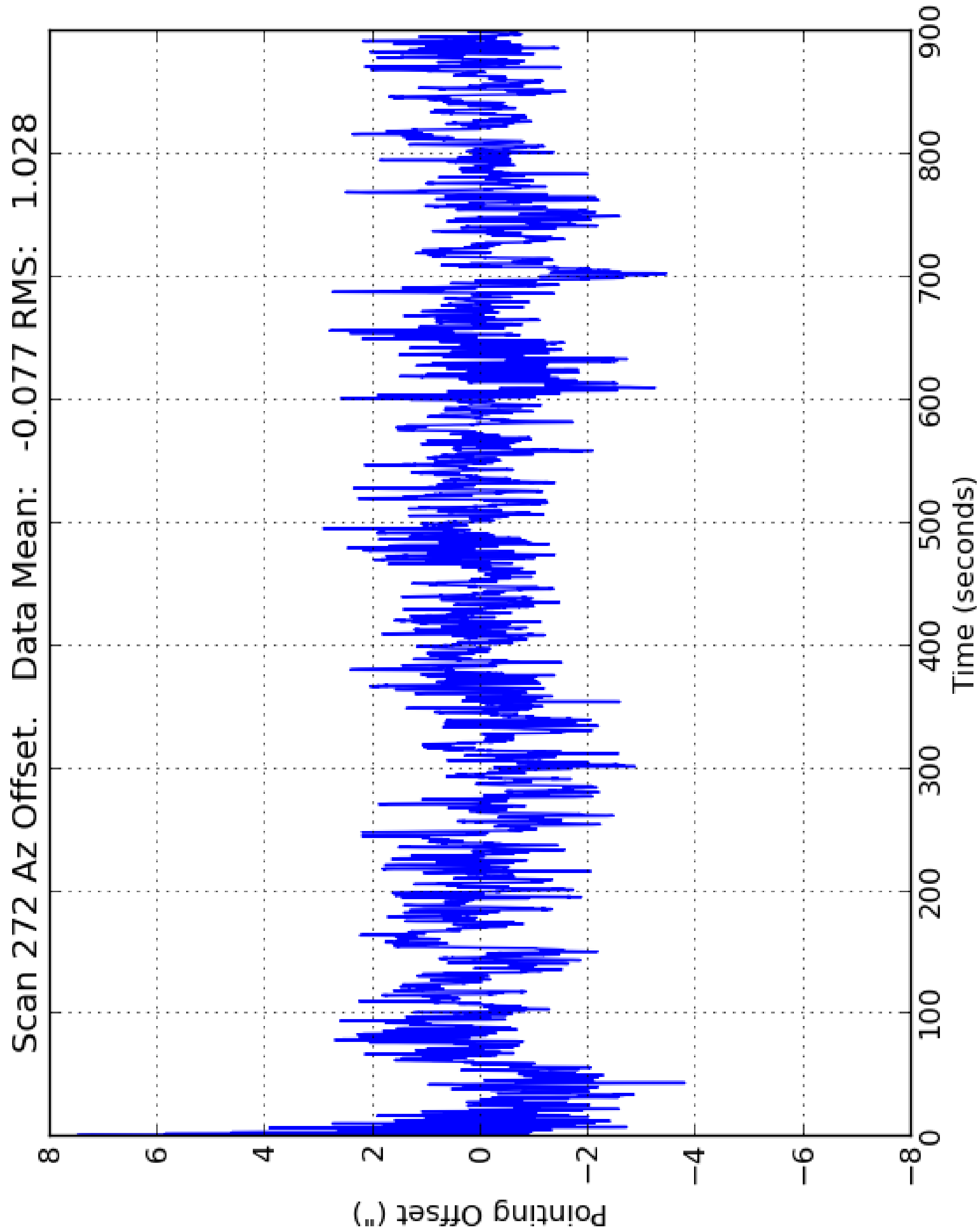


Fig. C11.— Half-power tracking data for scan 272